WASHINGTON UNIVERSITY
SEVER INSTITUTE OF TECHNOLOGY
DEPARTMENT OF CIVIL ENGINEERING

ABSTRACT

CONTROL OF A MOVING OSCILLATOR ON AN ELASTIC CONTINUUM

by Diego Giraldo

ADVISOR: Professor Shirley J. Dyke

December 2002
St. Louis, Missouri

An oscillator traversing an elastic continuum, often referred to as the moving-oscillator problem, is representative of many common engineering systems. A clear example of such a system in the civil engineering field is a vehicle crossing a bridge. Due to the dynamic interaction between the two subsystems, vibrations generated as the vehicle traverses the continuum cause deflections which may be significantly larger than those generated when such interaction is neglected. The goal of this thesis is to develop a control system that can reduce the dynamic responses of the combined system. A series expansion is used to model the continuum, which, when combined with a single degree of freedom oscillator, results in a time-varying, linear model describing the dynamics of the coupled system. Three different control techniques are considered: passive, active, and semiactive. These techniques will be applied and evaluated in terms of their ability to reduce the dynamic response of the continuum and the oscillator. A tracking control algorithm, that uses accelerations of both the continuum and the oscillator for feedback, is used to calculate the optimal control action. The results indicate that the response of the system with semiactive control approaches that of an active control, while using significantly less power. The controllers both outperform a passive control system.

To those who are always by my side: my family and my friends.

Contents

Tables

Figures

Acknowledgments

Special thanks to Dr. Shirley Dyke for her support and patience during all this period. Without her ideas, critics, and unscheduled help, this thesis would have never been a reality.

Thanks to Juan Caicedo for his friendship and support in my life and my research.

Thanks to Dr. Osamu Yoshida for his help and advice when it was about the “Control Systems” world. Thanks to Dr. Lawrence Bergman and all his associates who have worked to develop the mathematics behind the Moving-Oscillator problem.

Thanks to my family and friends.

Chapter 1

Introduction

The behavior of an elastic continuum excited by a moving oscillator is of great interest for a variety of engineering applications [23, 35]. In the civil engineering field for instance, the behavior of highway and railway bridges with a moving vehicle can clearly be modeled using this approach. The interacting dynamics of the bridge and the vehicle can increase the static response of the system dramatically, making this phenomenon important to consider in bridge design [7]. Other applications can also be found in the mechanical and aerospace fields.

Over the years, several mathematical models have been used to simulate the behavior of this system. The first and most basic representation neglects all dynamics and coupling between the oscillator and the continuum, reducing the response of the latter to a simple static deflection due to the mass of the oscillator. Using this approach, the deflection of the continuum is described by a polynomial whose coefficients change depending on the position of the load.

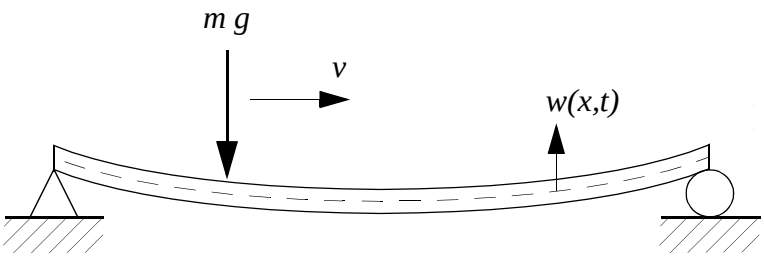

FIGURE 1-1. Moving force model.

More recently, the vehicle has been modeled as a moving force (see Fig. 1-1), producing a dynamic response of the continuum but neglecting both the inertia of the vehicle and the dynamics of its suspension. This model was clearly a step forward from calculating only the static deflections for different positions of the load, but was misrepresenting the dynamic interaction of the two subsystems. To improve upon this model, researchers proposed a moving mass rather than a simple moving force (see Fig. 1-2). This approach takes into account the changing mass distribution of the system but does not necessarily represent its real behavior as the dynamic coupling of the oscillator and the continuum is still neglected.

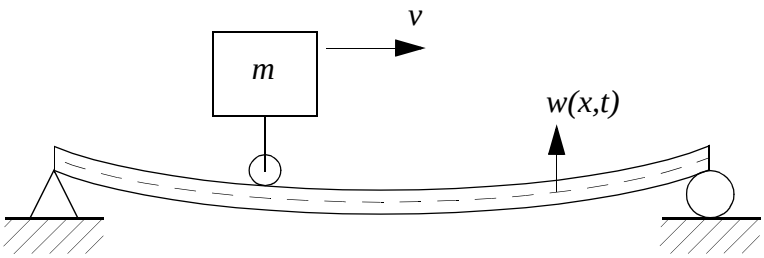

FIGURE 1-2. Moving mass model.

It was only in the late 1990s, that the development of new methods for analyzing the moving oscillator problem has overcome this limitation (see Fig. 1-3). Pesterev and Bergman [23] showed that this coupled system could be described by a time-varying system of linear equations. That is, the coefficient matrices vary as the oscillator moves along the length of the continuum. In the limiting case, this model has been shown to approach the solution to the moving mass problem [31, 32]. Results have indeed shown that the dynamic response of the coupled system may be significantly larger than the static response alone.

In these methods the response of the continuum is expressed as a Taylor series expansion. The convergence of this approach is satisfactory when trying to approximate continuous functions such as the displacement of the continuum. However, because the

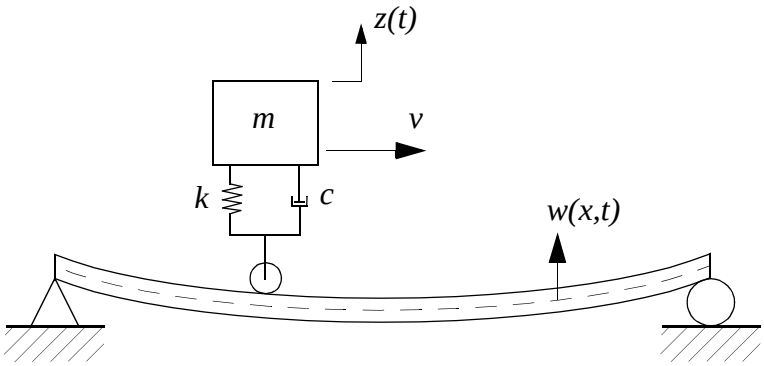

FIGURE 1-3. Moving-oscillator model.

oscillator is a point load, the distribution of shear forces is a non-continuous function, whereas the distribution of bending moments does not have a continuous derivative. Therefore, a series expansion alone is inadequate to represent the stress distribution along the continuum.

The moving oscillator model may be employed to study a variety of real-world systems. Cable transportation materials [35], high-speed precision machining [3, 17, 18], and magnetic hard drives [14, 15], are some of those applications. In civil engineering, it may represent a vehicle crossing a bridge, capturing the effects of their interaction. In this case, the characteristics of the load are determined by the mass of the vehicle, its suspension, and its velocity. Under certain common conditions, this interaction can cause significant dynamic responses producing an important source of damage and fatigue. With 900-billion ton-miles of commercial traffic traversing highways and highway bridges each year, this may have a significant effect on the lifetime of a bridge. Fifteen percent of bridges in the U.S. are classified as structurally deficient by the Federal Highway Administration (Bureau [2]; see also: *www.fhwa.dot.gov*). Controlling the effects of this vehicle-bridge interaction has the potential to significantly increase the service life of bridges.

Although this study may be applied to several types of distributed parameter systems such as non-continuous strings, the focus of this thesis is to apply control techniques to the specific case of a vehicle crossing a bridge. For this reason, a continuous beam is selected as the continuum. Moreover, because the shear deformation does not greatly affect the dynamic response of a beam, an Euler-Bernoulli beam model is employed.

1.1 Control Strategies

This thesis considers the use of several techniques for controlling the dynamic response of the system as the oscillator traverses the continuum. However, the total response of the system has both static and dynamic components. The goal herein is to apply a control action that forces the system to behave as if only static forces were being applied, minimizing the vibration produced mainly by the interaction between the two independent subsystems.

The control force is in all cases applied with a device placed in parallel with the spring and dashpot comprising the suspension of the moving oscillator. The fact that the actuator moves along the continuum makes the problem more challenging because the controllability of the variables is time dependent [12]. For instance, no control action can be applied to the continuum while the oscillator (carrying the control device) has not entered the beam, or has left it already. This controllability reaches its maximum value when the oscillator is at the midspan.

The first technique considered is active control. For over two decades, research and applications of this type of control systems to civil structures has been growing rapidly [29]. Active control systems operate by using external energy supplied by actuators to impart forces to the structure [5]. The appropriate control action is determined based on measurements of the structural responses. Because energy is input to the structure, an

active actuator combined with a faulty algorithm can potentially drive the system unstable, constituting one of the main limitations of this type of control.

Because of its capabilities, when applied to the vehicle-bridge model, a well designed active control system is expected to perform efficiently. The actuator for this case is considered to be ideal, and can instantaneously and precisely supply any control force. The optimal force at any time is calculated by an H_2/LQG control algorithm based on acceleration feedback [5, 9, 10]. These accelerations are measured with sensors located at certain points of the beam and the oscillator.

Two semiactive control designs are considered in this study. Unlike actuators used in active control, a semiactive device is unable to input energy to the structural system [6, 16]. The idea is to modulate the dissipation of energy with a damper whose properties can be changed in time so that optimal performance is achieved. A semiactive actuator is capable of producing tension and compression control forces, but can only do so when the velocity of its stroke is opposing the force (i.e. dissipative).

Several investigators have studied the suitability of this class of devices and have found them to be effective in reducing the response of structures to different dynamic loads [6, 11]. One of the most important advantages of semiactive control is that it requires much less power than active control. The reason for this difference lies in the fact the semiactive devices only react to the motion of the structure, dissipating energy in a controlled way. Moreover, because of its incapacity to introduce non-dissipative forces to the system, semiactive control systems are intrinsically stable (in the bounded input - bounded output sense).

Even though the power required by active and semiactive systems is very different, the performance of semiactive systems can, in many cases, approach that of the active control and, sometimes, even surpass it [8, 34]. However, these devices behave nonlinearly,

providing an additional challenge in the control design. A clipped optimal control algorithm is used to determine the control action.

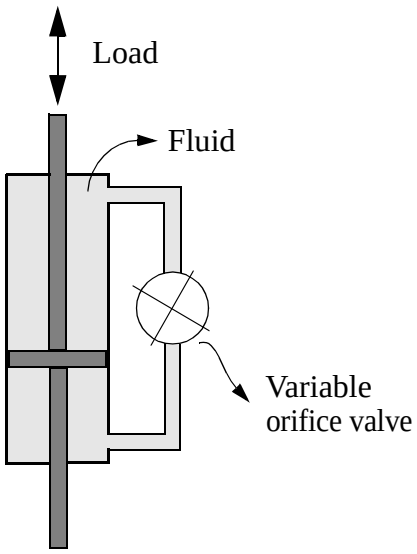

FIGURE 1-4. Schematic of a variable-orifice damper.

Hydraulic dampers with variable orifice and magnetorheological (MR) dampers are the semiactive devices considered in this thesis. Dampers with a variable orifice were some of the first devices developed for semiactive control. This class of dampers dissipate energy as oil is forced through a controllable valve, and thus controllable forces are generated (see Fig 1-4). Karnopp [16] described several possible configurations for the hydraulics of these dampers and some of their advantages and disadvantages. Because of the rapid dynamics of these devices compared to that of the vehicle-bridge system, it can be assumed that the damper can reach any desired damping coefficient very quickly.

Magnetorheological dampers (see Fig 1-5) have also been proven to be effective in civil structures [8, 11, 34]. These devices also require minimum power while generating large forces. MR-dampers take advantage of the controllable properties of MR fluids. When exposed to a magnetic field, MR fluids can reversibly change from a free-flowing, linear viscous fluid, to a semisolid with a controllable yield strength in milliseconds [5].

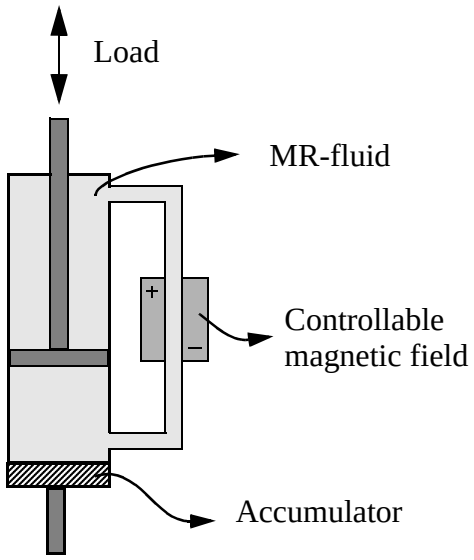

FIGURE 1-5. Schematic of an MR-damper.

One of the limitations of these control techniques is the amount of information that is required to identify the optimal control action. Some of this information can easily be obtained from the properties of the continuum and the oscillator, and do not change with time. However, some other required data need more attention. For instance, it is assumed here that the position of the oscillator as it crosses the continuum is precisely known at any time, as well as accelerations of the oscillator and certain points of the beam.

The data acquisition and computational effort are important factors that increase the cost of these kind of applications. To justify this moderate increase, it is important to verify the advantages of the performance of those techniques compared to that of the passive control systems that need neither the data nor the calculations of optimal control action. Therefore, two passive control techniques are applied and discussed. First, a viscous damper is applied. A viscous damper could be referred as the passive stage of the hydraulic damper of variable orifice, if no modification is done to its properties. Moreover, the performance of the system with an MR-damper in a passive mode is also analyzed and compared to all active and semiactive control performances.

1.2 Case Studies

Several cases of initial conditions and disturbance are considered as they may represent real conditions in this type of system. By applying several sets of conditions and comparing the performance of all control techniques, the robustness of each technique is tested. At first it is assumed that the beam has a perfect surface and is at rest when the oscillator enters from the left side, traveling at a constant speed with no vertical motion. Then a set of initial conditions is imposed on the system, simulating a previous excitation of the beam by another oscillator. In a third case, an imperfection in the surface of the bridge is considered. This imperfection (bump) introduces a disturbance that affects both subsystems at that particular point as the oscillator enters. In this case, both the initial conditions and non-perfect surface of the beam are considered simultaneously.

1.3 Configuration

In the case of a vehicle and bridge, Fig. 1-6 shows two possible configurations for applying such a control system. Both configurations use wireless technology for sending and receiving data in real time. Several authors have been researching applications in this field [20]. Bluetooth wireless networking, wireless hubs, and even global positioning are some of the options. While these methods are all still under development, wireless sensors are already available and cost is the main factor in choosing among them.

The configuration shown in Fig. 1-6b may be expected to be more reliable from the networking point of view. This configuration does not require a transmitter on each sensor placed on the bridge, lowering not only the risk of a cut in the transmission but also in the cost of installation.

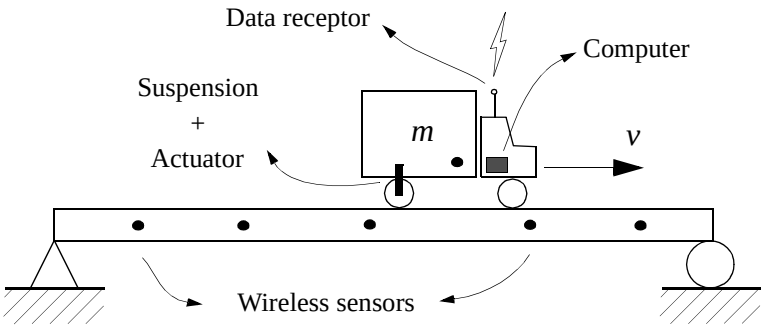

a) Wireless sensors on the bridge

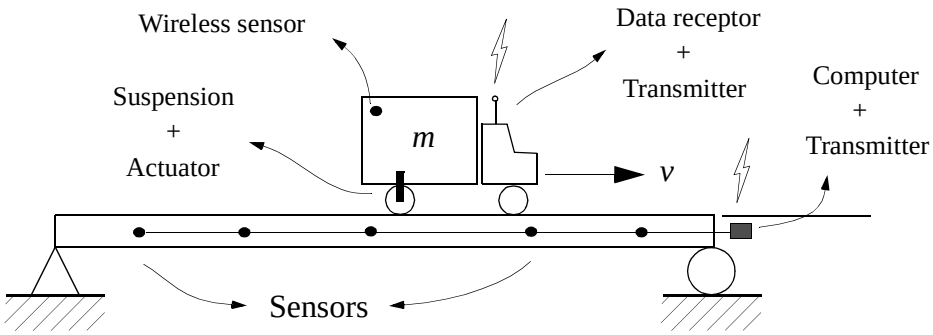

b) Wireless sensor on the vehicle

FIGURE 1-6. Possible configurations.

1.4 Overview

In this thesis several control techniques are considered to reduce the dynamic response of the moving-oscillator problem. A numerical example is created and simulated on the computer, allowing for a direct comparison of all control designs. Several cases of initial conditions and disturbance are considered to compare the robustness and capabilities of those techniques. The methodology and purpose of each chapter is explained in the following paragraphs.

Chapter 2 is devoted to the description of the mathematical model used to describe the dynamics of the system. At first, the homogeneous solution of the continuum by itself is

found, obtaining its natural frequencies and mode shapes. Then, the time response is expressed as a series expansion of those mode shapes and a set of time-dependent coefficients. The resulting time-dependent second order differential equations are rearranged in a single state space model.

Chapter 3 provides a background on the type of control devices used in this work. Although the dynamics and limitations of the active device are neglected (for comparison purposes), these parameters are accounted for and explained for both of the semi-active actuators. The algorithms used to calculate the optimal control action applied by each device are discussed in this chapter. Each of these algorithms is based on optimal control theory using a linear quadratic cost function and acceleration feedback. Moreover, because the main objective is to simulate the static behavior of the system, all control algorithms must know in advance this response in order to track its path. This "tracking signal" is also calculated in this chapter.

To verify the efficacy of the tracking control algorithms developed in Chapter 3, a simplified model is created in Chapter 4. A much simpler model facilitates testing several possible alternatives for tracking control design. Both the variable controllability of the response, and the time dependability of the system were neglected. For this reason, an excellent performance of the tracking control algorithm was pursued to proceed and apply the design to the much more complex moving-oscillator problem. Both the model and the results of controlled and uncontrolled cases are discussed here.

Chapter 5 provides a numerical example of the moving oscillator problem. The characteristics of the beam and the oscillator for this example were selected specifically to simulate the behavior of a simply supported bridge traversed by a vehicle. This chapter describes three different cases of initial conditions and disturbance under which the system is tested. The evaluation parameters needed to properly compare the behavior of all

control techniques are defined and mathematically described. The results of all control techniques are provided and discussed.

Chapter 6 is reserved for conclusions of the research and provides some possibilities for future studies.

Chapter 2

Mathematical Approach

The success of a controller depends strongly on the adequacy of the model used to represent the actual phenomenon. A mathematical model that does not represent the physical behavior of the system well, may lead to an ineffective control strategy and possibly instability. The model used in this thesis was developed by Pesterev and Bergman in 1997 [23], and expresses the response of the continuum as a Taylor series expansion of its eigensolution. The advantage of this model is that in addition to accounting for the dynamics of the two subsystems, the model also includes coupling between them. Additionally, it is a low order model, which is highly appropriate for control design.

In this chapter the differential equations that govern the coupled system are derived and expressed in state space form. The most important reason to use this notation is the advantages that it offers from the control design point of view. This issue will become clear in Chapter 3 which discusses the background of control systems design and proposes a controller for the moving oscillator problem.

To simplify the equations used to describe the dynamics of the continuum and the oscillator in the first sections of this chapter, the terms that involve their damping characteristics are neglected. These terms however, are displayed in the state space model developed in the ending sections of the chapter, and are also accounted for in the numerical simulations described in later chapters.

One challenge in the control system design introduced in the moving oscillator problem is the fact that the properties of the combined system, such as natural frequencies and mode shapes, vary as the oscillator traverses the continuum. When represented in a state space model, this means that the coefficient matrices are time dependent. The differential equations describing this phenomenon are developed herein.

2.1 Equation of Dynamic Equilibrium

Figure 2-1 shows a straight, simply supported beam with flexural rigidity EI and mass ρ per length that are functions of x. The beam is subjected to a time dependent distributed load $P(x, t)$ perpendicular to its axis.

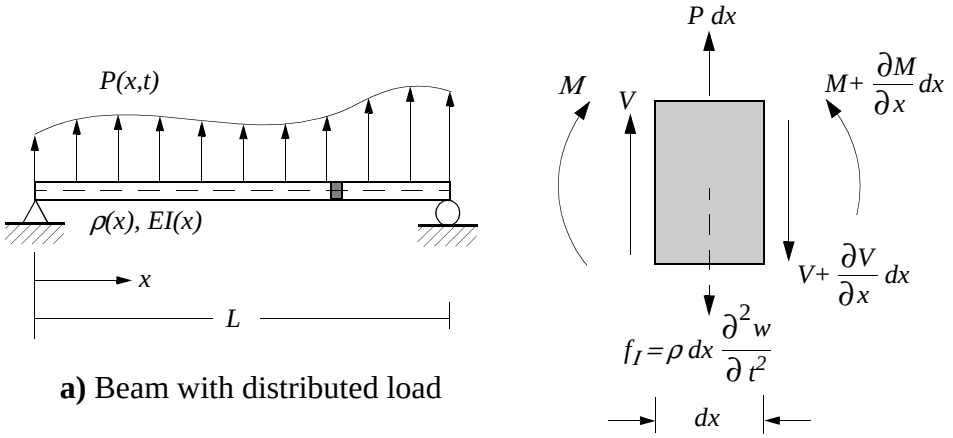

a) Beam with distributed load

b) Internal equilibrium

FIGURE 2-1. Internal equilibrium of an elastic continuum with a distributed load.

The increment on the shear force for each portion of the beam is given by the expression

$$\frac{\partial V}{\partial x} = P(x, t) - \rho(x)\frac{\partial^2}{\partial t^2}w(x, t), \qquad (2\text{-}1)$$

where $w(x, t)$ is the vertical deflection of the continuum for any given point and time. It is well known that the shear force and bending moment for every portion of the beam are defined as

$$V(x) = \frac{\partial M(x)}{\partial x} \quad \text{and} \quad M(x) = EI\frac{\partial^2}{\partial x^2}w(x, t). \tag{2-2}$$

Substituting the expressions given in Eq. (2-2) into Eq. (2-1), the following dynamic equilibrium equation is obtained

$$\rho(x)\frac{\partial^2}{\partial t^2}w(x, t) + \frac{\partial^2}{\partial x^2}\left(EI(x)\frac{\partial^2}{\partial x^2}w(x, t)\right) = P(x, t). \tag{2-3}$$

Assuming a uniformly distributed mass and an unvarying stiffness along the continuum, Eq. (2-3) may be simplified to

$$\rho\frac{\partial^2}{\partial t^2}w(x, t) + EI\frac{\partial^4}{\partial x^4}w(x, t) = P(x, t). \tag{2-4}$$

2.2 Homogeneous Solution

From the homogeneous solution of the equation of equilibrium (2-4) we can obtain the characteristics of the beam itself, specifically, natural frequencies and mode shapes. A brief overview of the this solution is provided as follows [4]. The input force is set to zero

$$\rho\frac{\partial^2}{\partial t^2}w(x, t) + EI\frac{\partial^4}{\partial x^4}w(x, t) = 0. \tag{2-5}$$

It is assumed that the response of the continuum is given by the product of two different expressions, one of them being a function of time only, and the other a function of the position along the beam. That is

$$w(x, t) = \phi(x)\, q(t). \tag{2-6}$$

This method is called *separation of variables* and is widely used in solving partial differential equations such as Eq. (2-5). Introducing this new expression into Eq. (2-5)

$$\rho\phi(x)\ddot{q}(t) + EI\phi''''(x)q(t) = 0, \tag{2-7}$$

where the dot ($\dot{}$) represents a derivative with respect to time and the prime ($'$) means the derivative with respect to x. Equation (2-7) can be reorganized as

$$-\frac{\ddot{q}(t)}{q(t)} = \frac{EI\phi''''(x)}{\rho\phi(x)}. \tag{2-8}$$

Note that the left side of Eq. (2-8) depends on time only, while the right side depends on the variable x. It is known that when two expressions that depend on two different variables are equal to each other, they must be equal to a constant. That is

$$-\frac{\ddot{q}(t)}{q(t)} = \frac{EI\phi''''(x)}{\rho\phi(x)} = \omega_n^2, \tag{2-9}$$

and therefore, two ordinary differential equations of second order can be obtained

$$\phi''''(x) - \frac{\rho\,\omega_n^{\,2}}{EI} = 0 \tag{2-10}$$

$$-\ddot{q}(t) + \omega_n^2\, q(t) \;=\; 0\,. \tag{2-11}$$

Solving Eq. (2-10) gives us the natural frequencies and mode shapes of the continuum. However, these characteristics depend on the selected boundary conditions. As mentioned before, this thesis focuses on the case of a simply supported beam. Knowing then that the displacements and bending moments at both ends are equal to zero, the following natural frequencies and mode shapes are obtained [4]

$$\omega_n \;=\; \frac{n^2\pi^2}{L^2}\sqrt{\frac{EI}{\rho}} \qquad \text{for} \quad n \;=\; 1, 2, 3, \ldots \tag{2-12}$$

$$\phi_n(x) \;=\; C_1 \sin(n\pi) \qquad \text{for} \quad n \;=\; 1, 2, 3, \ldots \tag{2-13}$$

Eq. (2-13) gives us the sinusoidal mode shapes as shown in Fig. 2-2.

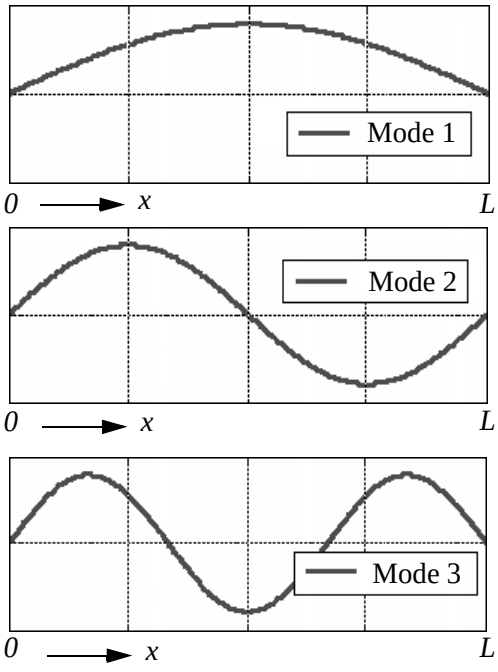

FIGURE 2-2. First three mode shapes of the continuum

Because the solution to the equation of equilibrium is not unique and can be expressed with several independent terms, it is true that a better approximation to the total response is given by a linear combination of those modal functions. That means

$$w(x, t) = \sum_{n=1}^{N} \phi_n(x) q_n(t) . \tag{2-14}$$

2.3 Moving Oscillator Problem

Figure 2-3 shows the specific case in which the distributed load is replaced by a moving oscillator that traverses the beam at a constant velocity.

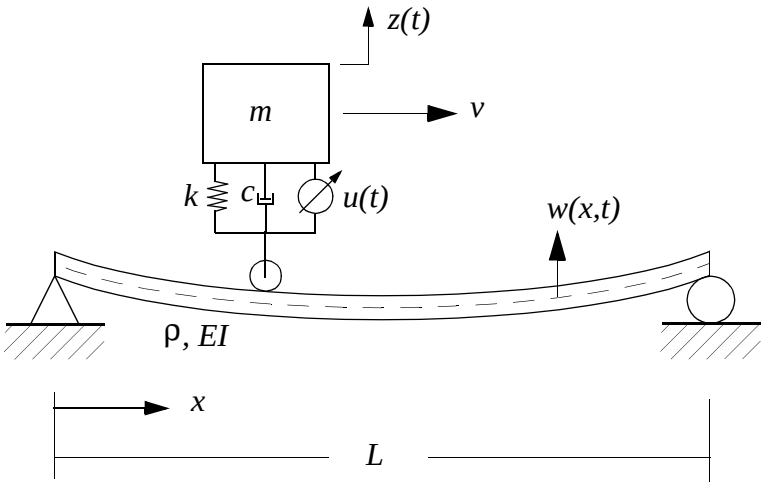

FIGURE 2-3. Linear oscillator traversing an elastic continuum.

The characteristics of the oscillator are given by m which represents the mass, k the stiffness of its suspension, c the damping coefficient, v its velocity, and $z(t)$ the vertical displacement from its equilibrium position. The characteristics of the continuum are ρ, which represents its mass per unit length, EI its flexural rigidity, L its total length,

and $w(x, t)$ the displacement of every point at any time. The force applied by the control device is expressed as $u(t)$. For this particular case, Eq. (2-4) becomes

$$\rho\left(\sum_{n=1}^{N}\phi_n(x)\ddot{q}_n(t)\right) + EI\frac{\partial^4}{\partial x^4}\left(\sum_{n=1}^{N}\phi_n(x)q_n(t)\right) = \left[H(t) - H\left(t-\frac{L}{v}\right)\right][\delta(x - v_i(t-t_i))](f_i(t) - mg), \qquad (2\text{-}15)$$

where $H(t)$ is the heavyside function, $\delta(\ )$ is the dirac delta, x is the coordinate along the continuum, and $f(t)$ is the force applied by the suspension of the oscillator. If we restrict our attention to the specific time when the oscillator is traversing the continuum (i.e. $t \in [0, L/v]$), then Eq. (2-15) can be written as

$$\rho\left(\sum_{n=1}^{N}\phi_n(x)\ddot{q}_n(t)\right) + \omega_n^2\left(\sum_{n=1}^{N}\phi_n(x)q_n(t)\right) = \delta(x - vt)(f(t) - mg) \qquad (2\text{-}16)$$

Considering the moving oscillator alone, the equation governing its motion is

$$m\,\ddot{z}(t) + f(t) = 0. \qquad (2\text{-}17)$$

At each time, the force applied to the sprung mass and the beam is given by

$$f(t) = k\,(z(t) - w(vt, t)) + u(t) \qquad (2\text{-}18)$$

If Eq. (2-16) is multiplied by $\phi_n(x)$ and integrated over time, the orthogonality properties of the modes can be used to simplify this expression and reduce its dependency to time only. The resulting equation involves the generalized coordinates of the continuum [23]

$$\ddot{q}_n(t) + \omega_n^2\ q_n(t)\ =\ C_1\sqrt{\frac{\rho L}{2}}\ \phi_n(vt)\ (f(t) - mg) \qquad \text{for } n\ =\ 0, 1, 2, \ldots, N \qquad (2\text{-}19)$$

C_1 is selected so that the coefficient of the right side of Eq. (2-19) is equal to the unit

$$C_1\ =\ \sqrt{\frac{2}{\rho L}}, \qquad (2\text{-}20)$$

and Eq. (2-19) can be rewritten as

$$\ddot{q}_n(t) + \omega_n^2\ q_n(t)\ =\ \phi_n(vt)\ (f(t) - mg) \qquad \text{for } n\ =\ 0, 1, 2, \ldots, N \qquad (2\text{-}21)$$

Using Eq. (2-14) in Eq. (2-18), the following expression for the force is obtained

$$f(t)\ =\ k\left(z(t) - \sum_{j\,=\,1}^{N} \phi_j(vt) q_j(t)\right) + u(t) \qquad (2\text{-}22)$$

Eq. (2-22) can be used in Eqs. (2-17) and (2-21), obtaining the following system of coupled expressions

$$\ddot{z}\ =\ \phi_n(vt)\ \frac{k}{m}\ z\ (t) - \phi_n(vt)\ \frac{k}{m} \sum_{i\,=\,1}^{N} \phi_j(vt) q_j(t) - \phi_n(vt)\ g + \frac{1}{m}\phi_n(vt) u(t) \qquad (2\text{-}23)$$

$$\ddot{q}_n(t)\ =\ -\omega_n^2\ q_n(t) + \phi_n(vt) k\ z(t) - \phi_n(vt) k \sum_{i\,=\,1}^{N} \phi_j q_j(t)(tv)$$
$$- \phi_n(vt) mg + \phi_n(vt) u(t) \qquad \text{for } n\ =\ 0, 1, 2, \ldots, N \qquad (2\text{-}24)$$

Eqs. (2-23) and (2-24) can be solved to determine the response of the coupled system. Note that the coefficients of these equations are time-varying, and the equations are linear.

2.4 State Space Model

Defining the state vector $\mathbf{x} = \left[z\ q_1\ q_2\ \ldots\ q_N\ \dot{z}\ \dot{q}_1\ \dot{q}_2\ \ldots\ \dot{q}_N\right]^T$, and taking into account the damping characteristics of the two subsystems, we can rewrite Eqs.(2-23) and (2-24) in state space form as

$$\dot{\mathbf{x}} = \begin{bmatrix} \mathbf{0} & \mathbf{I} \\ \mathbf{G} & \mathbf{J} \end{bmatrix}\mathbf{x} + \begin{bmatrix} \mathbf{0} \\ \mathbf{H}_2 \end{bmatrix}u(t) + \begin{bmatrix} \mathbf{0} \\ \mathbf{H}_1 \end{bmatrix}mg = \mathbf{A}(t)\mathbf{x} + \mathbf{B}(t)u(t) + \mathbf{E}(t)(mg) \qquad (2\text{-}25)$$

where

$$\mathbf{G} = \left[\begin{array}{c|ccc} -\frac{k}{m} & \frac{k}{m}\phi_1(vt) & \ldots & \frac{k}{m}\phi_N(vt) \\ \hline k\phi_1(vt) & -\omega_1^2 - k\,\phi_1(vt)\phi_1(vt) & \ldots & -k\,\phi_1(vt)\phi_N(vt) \\ \vdots & \vdots & \ldots & \vdots \\ k\phi_N(vt) & -k\,\phi_N(vt)\phi_1(vt) & \ldots & -\omega_N^2 - k\,\phi_N(vt)\phi_N(vt) \end{array}\right], \qquad (2\text{-}26)$$

$$\mathbf{J} = \left[\begin{array}{c|ccc} -\frac{c}{m} & \frac{c}{m}\phi_1(vt) & \ldots & \frac{c}{m}\phi_N(vt) \\ \hline c\phi_1(vt) & -2\,\omega_1\,\zeta_1 - c\,\phi_1(vt)\phi_1(vt) & \ldots & -c\,\phi_1(vt)\phi_N(vt) \\ \vdots & \vdots & \ldots & \vdots \\ c\phi_N(vt) & -c\,\phi_N(vt)\phi_1(vt) & \ldots & -2\omega_N\,\zeta_N - c\phi_N(vt)\phi_N(vt) \end{array}\right]. \qquad (2\text{-}27)$$

$$\mathbf{H}_1 = \begin{bmatrix} 0 \\ -\phi_1(vt) \\ \vdots \\ -\phi_N(vt) \end{bmatrix} \quad \text{and} \quad \mathbf{H}_2 = \begin{bmatrix} -\frac{1}{m} \\ \phi_1(vt) \\ \vdots \\ \phi_N(vt) \end{bmatrix}, \tag{2-28}$$

where c represents the damping coefficient of the oscillator, and ζ_n the damping ratio of the n^{th} mode of the continuum. The output equation is selected to include the states, as well as their first and second derivatives

$$\mathbf{y} = \begin{bmatrix} \mathbf{I} & \mathbf{0} \\ \mathbf{0} & \mathbf{I} \\ \mathbf{G} & \mathbf{J} \end{bmatrix} \mathbf{x} + \begin{bmatrix} \mathbf{0} \\ \mathbf{0} \\ \mathbf{H}_2 \end{bmatrix} u(t) + \begin{bmatrix} \mathbf{0} \\ \mathbf{0} \\ \mathbf{H}_1 \end{bmatrix} mg = \mathbf{C}(t)\mathbf{x} + \mathbf{D}(t)u(t) + \mathbf{F}(t)(mg) \tag{2-29}$$

where $\mathbf{y} = \begin{bmatrix} z & q_1 & q_2 & \dots & q_N & \dot{z} & \dot{q}_1 & \dot{q}_2 & \dots & \dot{q}_N & \ddot{z} & \ddot{q}_1 & \ddot{q}_2 & \dots & \ddot{q}_N \end{bmatrix}^T$.

2.5 Summary

The mathematical approach used to model the behavior of the continuum and the oscillator and their dynamic interaction has been developed in this chapter. First the equilibrium equations were derived. Then the homogeneous solution of the continuum alone was found, obtaining natural frequencies and mode shapes. A series expansion of those eigensolutions, was used to represent the displacement of the beam as the oscillator traverses the continuum. The coupled equations of motion were then set and expressed in state space notation.

Chapter 3

Control Background

The linearity of the system and the fact that the input force introduced by the oscillator can be expressed as a sum of two terms (see Chapter 2, Eq. (2-16)) indicates that the response of the entire system can be divided into two independent components. Pesterev and Bergman derived the equations to solve these two components and called them the moving-force and the elastic-force solutions of the moving oscillator problem [25]. However, when the oscillator travels at a low velocity, the moving-force solution approaches the solution based on static deflections. In this study, only cases where this is true are considered, and the moving-force solution will be referred to as the pseudostatic response.

It is obvious that to reduce the pseudostatic response, it is necessary to change the properties of the beam itself, such as stiffness or boundary conditions. The dynamic component, however, can be reduced with a number of mechanisms. For instance, tuned-mass dampers or active mass drivers located at certain points of the beam are options to achieve this objective. The method proposed in this thesis comprises a device attached to the suspension of the oscillator and a control algorithm that determines the optimal action to be taken. Depending on the type of actuator, this control action varies from a commanded force for active control, a damping coefficient for a damper of variable orifice, or a commanded voltage for an MR-damper. The device, in all cases, applies forces of equal magnitude but opposite directions to the beam and the oscillator.

It is important to note that the controllability of the system is time dependent. The reason for this dependence is due to the fact that the control device moves along the continuum, changing its capability to interact with it. For instance, the controllability of the first mode of the beam reaches its maximum value when the oscillator is placed at the midspan, and decreases as the oscillator moves away from this point. Similarly, the controllability of the second mode has two maximum values at one quarter and three quarters of the span, having a zero value in the midspan. Obviously, no control can be applied on any mode of the continuum before the oscillator enters it, or after it has finished crossing it. The controllability of the oscillator's response also changes as it traverses the continuum, although to a lesser degree. The controllability of this response reaches its minimum value (not zero) at the midspan, and has a maximum value whenever the oscillator is off the bridge.

3.1 Device Models

An adequate understanding of the behavior of the control device is a very important element when designing a control system. Its capacity to supply a commanded action and the way it performs that action are two important factors to be accounted for. However, the influence of these factors on the design, depend not only on the characteristics of the actuator itself, but also on the dynamics of the system.

Three devices are modeled and tested in this study: one for active control design and two more for semiactive and passive control designs. The main assumptions, characteristics and equations describing their capacity and dynamics are explained in the following sections.

3.1.1 Active Actuator

It is always desirable for an actuator to have a quick dynamic response relative to that of the system being controlled, and to be able to apply any force commanded, without

restrictions of magnitude. When these two conditions are met, it is sometimes reasonable to neglect both actuator dynamics and control-structure interaction. The actuator for the active control design is assumed to be an ideal device. Thus, any force commanded by the control algorithm is applied exactly as needed. Both compression and tension forces are required by the system. In real applications, several devices such as hydraulic actuators are capable of producing forces of the same magnitude required by this application. However, their dynamics are not negligible and would have to be accounted for when applied to the moving-oscillator problem.

Assuming that the actuator is an ideal device allows us to investigate the best performance that can be obtained with active control, and compare its results to those obtained with other control designs. This facilitates a study which will determine the potential for application of this technology.

3.1.2 Variable Orifice Damper

Dampers with a variable orifice generate controlled responses as oil is forced through a controllable valve [26]. Because of the rapid dynamics of these valves compared to that of the vehicle-bridge system, it is assumed that this actuator has an ideal behavior. An ideal semiactive device is a damper whose properties can be changed instantaneously to any desired value. Figure 3-1 displays the mechanical model used for this device.

The force generated by the device is

$$f(t) = c(t)\,\dot{y}(t), \tag{3-1}$$

where $y(t)$ is the stroke and $c(t)$ is the damping coefficient that can be changed to any desired value commanded by the control algorithm.

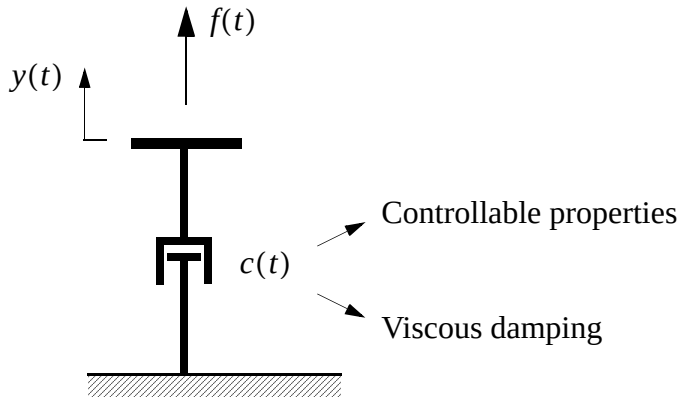

FIGURE 3-1. Mechanical model of a damper with variable orifice

To minimize the vibration generated by uneven roads, most commercial vehicles use viscous dampers which can be modeled using Eq. (3-1) and a constant damping coefficient. For this reason, the behavior of a bridge, when traversed by a vehicle, is expected to behave similar to the moving-oscillator model with this device.

Although theoretically the forces generated by this model are unlimited, it is also true that there is a limited force capacity to each device. To account for this bound, the model is limited to certain value of maximum force and will generate this value whenever the theoretical model surpasses it. Thus the model is not linear for large velocity motions.

3.1.3 Magnetorheological Damper

Magnetorheological (MR) fluids can reversibly change from a free-flowing fluid, to a semisolid with a controllable yield strength, when exposed to a magnetic field. MR-dampers take advantage of these properties to generate controllable forces.

MR-dampers have an inherent nonlinear behavior that researchers have tried to identify and simulate with different mathematical models. These models, however, are accurate

for a limited set of devices, depending on their size and hysteretical behavior. One of the simplest and more accurate models is the Bouc-Wen model of Fig. 3-2, which was developed and shown to precisely predict the behavior of a prototype shear-mode MR-damper over a wide range of inputs in a set of experiments [8, 33].

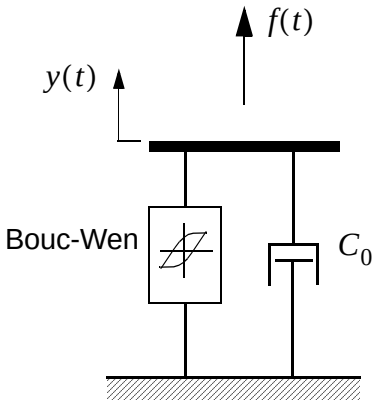

FIGURE 3-2. Mechanical model of MR-damper.

This model is also expected to be appropriate for modeling of a full-scale MR damper [5, 6, 8]. It combines a viscous damping force with a nonlinear Bouc-Wen force. The force applied by this MR-damper is given by the expression

$$f = C_o \dot{y} + \alpha z, \tag{3-2}$$

where y is the stroke of the device and z is the evolutionary variable that accounts for the history of the response of the damper. z is defined by the differential equation

$$\dot{z} = -\gamma |\dot{y}| z |z|^{n-1} - \beta \dot{y} |z|^n + A \dot{y}. \tag{3-3}$$

By adjusting the parameters of the model γ, β, n, and A, one can control the linearity in the unloading and the smoothness of the transition from the preyield to the postyield

region. The functional dependence of the device parameters on the effective voltage u is modeled as

$$\alpha(u) = \alpha_a + \alpha_b u \tag{3-4}$$

$$C_o(u) = c_{oa} + c_{ob} u . \tag{3-5}$$

Although the current driver circuit of the MR-damper introduces dynamics into the system, these dynamics are neglected. This means that it is assumed that the circuit provides any desired voltage to the MR-damper instantaneously. This assumption is reasonable when the dynamics of the system are much slower than the velocity of reaction of the circuit itself.

3.2 Control Design and Algorithms

As mentioned before, the main goal of this study is to minimize the dynamic response of the continuum as the oscillator traverses it. This means that no control action is taken to reduce the pseudostatic deflection of the beam generated by the mass of the vehicle. However, the states of the state space model developed in Chapter 2 do not make a distinction between the components of the total response due to static and dynamic loads. Therefore, if a control algorithm performs any action to reduce these states, this action will not only try to reduce the dynamic component of the response but also the static component.

Most control techniques applied in the civil engineering field focus on reducing the total response of the structure. Usually, to achieve this goal, a linear quadratic regulator that, by definition, drives the states to zero is used. However, because the control design applied in this study focuses on reducing the dynamic component only, a slightly different approach is used in this thesis. To apply this method, it is necessary to know what the

behavior of the system is when no dynamic interaction is present between the oscillator and the continuum. Then a control action is taken in order to approximate the response of the coupled system to that of the static behavior.

Thus, rather than a regulator, the problem of controlling the continuum-oscillator dynamic interaction then becomes a tracking problem in which the states are forced to follow the behavior of the pseudostatic response. Therefore, both the states related to displacements and the ones related to velocities are required in advance.

With the exception of the viscous damper, all devices described in Section 3.1 are commanded by algorithms that find the optimal control action to be taken by a particular device. Therefore, each of these algorithms has to account for the characteristics of the device in order to achieve the best possible response of the system. All algorithms and strategies used in this study are described in this chapter.

3.2.1 Passive Strategy

A passive control strategy does not need a control algorithm. It is obtained by placing a device that reacts to the motion of the system with certain properties that cannot be changed in time. Therefore, no data acquisition system or processing effort is needed. A passive strategy is used with two different devices in this study: viscous damper (set to a constant damping coefficient) and magnetorheological damper (with a constant voltage).

3.2.2 Tracking Signal

Green's formula is used to determine the static response of the continuum for any position of the oscillator. For a simply supported beam, this formula takes the form

$$G(x,\zeta) = \frac{mg}{6EI}\left((x-\zeta)^3 H(x-\zeta) - \frac{x^3(L-\zeta)}{L} - \frac{x(L-\zeta)^3}{L} + xL(L-\zeta)\right), \qquad (3\text{-}6)$$

where ζ represents the position of the oscillator, x the coordinate along the length of the continuum, m the mass of the oscillator, and g the gravitational force. Assuming the oscillator enters the beam at $t = 0$ with a constant velocity, Eq. (3-6) becomes

$$G(x, t) = \frac{mg}{6EI}\left((x - vt)^3 H(x - vt) - \frac{x^3(L - vt)}{L} - \frac{x(L - vt)^3}{L} + xL(L - vt)\right), \quad (3\text{-}7)$$

where v is the velocity of the oscillator. Eq. (3-7) is referred to as Green's pseudo-static formula because, even though it provides static deflections due to the mass of the oscillator, it is a time dependent function. In the hypothetical case in which the oscillator traverses the continuum at a constant velocity producing no other response than simply static deflections given by Green's formula, the velocity of each portion of the beam is given by its derivative with respect to time. This expression is

$$\begin{aligned}\frac{G(x, t)}{dt} = \frac{mg}{6EI}[&- vx^3\delta(x - vt) + 3vx^2 H(x - vt) - 3x^2v^2t\delta(x - vt) \\ &6v^2xtH(x - vt) - 3v^3xt^2\delta(x - vt) - 3v^3t^2H(x - vt) \\ &v^4t^3\delta(x - vt) + \frac{v}{L}x^3 + 2vLx - 6v^2xt + 3\frac{v}{L}xt^2\Big]. \quad (3\text{-}8)\end{aligned}$$

The output of Eqs. (3-7) and (3-8), however, are vertical deflections and velocities of the continuum respectively, whereas the states of the model developed in Chapter 2 do not represent these physical values. Instead, the states of the model represent the coefficients of the eigensolutions of the system. In theory, an infinite combination of those modes with the appropriate coefficients will approach exactly the solutions given by Green's formula and its derivative with respect to time. A limited number of modes is used to approximate the total response in this study.

Discrete values of Eq. (3-7), and the eigenmodes (given by Eq. (2-13)) are used to solve this problem numerically. The length of the beam is then divided into a number of sections j, whereas i periods of time are used. Thus, setting Eq. (2-14) equal to the discrete values of Green's formula, and expressing it in matrix form, the following expression is obtained

$$\begin{bmatrix} \begin{bmatrix} q_1(t_1) \\ q_1(t_2) \\ \vdots \\ q_1(t_i) \end{bmatrix} & \begin{bmatrix} q_2(t_1) \\ q_2(t_2) \\ \vdots \\ q_2(t_i) \end{bmatrix} & \cdots & \begin{bmatrix} q_N(t_1) \\ q_N(t_2) \\ \vdots \\ q_N(t_i) \end{bmatrix} \end{bmatrix} \begin{bmatrix} \begin{bmatrix} \phi_1(x_1) & \phi_1(x_2) & \ldots & \phi_1(x_j) \end{bmatrix} \\ \begin{bmatrix} \phi_2(x_1) & \phi_2(x_2) & \ldots & \phi_2(x_j) \end{bmatrix} \\ \vdots \\ \begin{bmatrix} \phi_N(x_1) & \phi_N(x_2) & \ldots & \phi_N(x_j) \end{bmatrix} \end{bmatrix}$$

$$= \begin{bmatrix} G(x_1, t_1) & \ldots & G(x_j, t_1) \\ \vdots & & \vdots \\ G(x_1, t_i) & \ldots & G(x_j, t_i) \end{bmatrix}, \qquad (3\text{-}9)$$

or,

$$\Gamma\, \theta = \mathbf{G} \qquad (3\text{-}10)$$

where $\begin{bmatrix} q_n(t_1) & q_n(t_2) & \ldots & q_n(t_i) \end{bmatrix}^T$ represents the vector containing the coefficients of the n^{th} mode at i times, and $\begin{bmatrix} \phi_n(x_1) & \phi_n(x_2) & \ldots & \phi_n(x_j) \end{bmatrix}$ is the x-dependent vector of the n^{th} eigenmode for all j sections of the beam. Because the discrete values of the eigenmodes (θ) and the pseudo-static formula ($\mathbf{G}$) are both known matrices that can be easily calculated based on the properties of the continuum, the problem is then reduced to that of finding the time-dependent coefficients q_n (Γ), from an overdetermined set of

linear equations. The least squares approximation is used to solved this problem by using a pseudo-inverse. Eq. (3-10) takes then the form

$$\Gamma = \mathbf{G}\,\theta^{+}, \tag{3-11}$$

where θ^{+} represents the pseudo-inverse of this non-square matrix. This approach is also applied to obtain the first derivative of the states ($\dot{q}_n(t)$) using the expression given in Eq. (3-8). The oscillator is assumed to have the same displacement and velocity of the continuum at the point is placed at any time, so that the relative distance between the two subsystems is constant.

Finally, for any time, the states to be tracked can then be grouped together in a vector as follows

$$\mathbf{x}_r = \left[z\ q_1\ q_2\ \ldots\ q_N\ \dot{z}\ \dot{q}_1\ \dot{q}_2\ \ldots\ \dot{q}_N\right]^T. \tag{3-12}$$

3.2.3 LQ Tracking Algorithm

The model developed in Chapter 2 is described by Eqs. (2-25) and (2-29), which can be rewritten as

$$\dot{\mathbf{x}} = \mathbf{A}\mathbf{x} + \mathbf{B}u + \mathbf{E}(mg) \tag{3-13}$$

$$\mathbf{y} = \mathbf{C}\mathbf{x} + \mathbf{D}u + \mathbf{F}(mg), \tag{3-14}$$

where the matrix coefficients are all time dependent. Defining an error vector $\mathbf{x}_e$ equal to the difference between the states of the system and the reference states as

$$\mathbf{x}_e = \mathbf{x} - \mathbf{x}_r, \tag{3-15}$$

and therefore

$$\mathbf{x} = \mathbf{x}_e + \mathbf{x}_r. \tag{3-16}$$

$$\dot{\mathbf{x}} = \dot{\mathbf{x}}_e + \dot{\mathbf{x}}_r. \tag{3-17}$$

Substituting Eqs. (3-16) and (3-17) into (3-13) yields

$$\dot{\mathbf{x}}_e + \dot{\mathbf{x}}_r = \mathbf{A}(\mathbf{x}_e + \mathbf{x}_r) + \mathbf{B}u + \mathbf{E}(mg), \tag{3-18}$$

which can be reorganized and expressed as

$$\dot{\mathbf{x}}_e = \mathbf{A}\mathbf{x}_e + \mathbf{B}u + \mathbf{E}(mg) + (\mathbf{A}\mathbf{x}_r + \dot{\mathbf{x}}_r). \tag{3-19}$$

An infinite horizon quadratic performance index is selected. This index has the form

$$J = \lim_{t_f \to \infty} \int_0^{t_f} (\mathbf{x}_e{}^T \mathbf{Q}\, \mathbf{x}_e + u^T \mathbf{R}\, u) dt, \tag{3-20}$$

where $\mathbf{Q}$ and $\mathbf{R}$ are the weighting matrices of the error and the control forces respectively. The goal is then to minimize the performance index so that the error is driven to zero and the system has a behavior as close as possible to the static behavior. To achieve this goal, the control law is of the form [1]

$$u(t) = -\frac{1}{2}\, \mathbf{R}^{-1}\mathbf{B}^T\, \lambda(t), \tag{3-21}$$

and the co-state equation is

$$\dot{\lambda}(t) = -\mathbf{A}^T\lambda(t) - 2\mathbf{Q}\mathbf{x}_e(t), \tag{3-22}$$

where the final condition is known, $\lambda(t_f) = 0$, and

$$\lambda(t) = \mathbf{P}(t)\mathbf{x}_e(t) \tag{3-23}$$

Differentiating Eq. (3-23) with respect to time yields

$$\dot{\lambda}(t) = \dot{\mathbf{P}}(t)\mathbf{x}_e(t) + \mathbf{P}(t)\dot{\mathbf{x}}_e(t). \tag{3-24}$$

Replacing $\lambda(t)$ of Eq. (3-21) by the expression given in Eq. (3-23)

$$u(t) = -\frac{1}{2}\mathbf{R}^{-1}\mathbf{B}^T\mathbf{P}(t)\mathbf{x}_e(t), \tag{3-25}$$

and substituting this into Eq. (3-19) one can obtain

$$\dot{\mathbf{x}}_e = \mathbf{A}\mathbf{x}_e - \frac{1}{2}\mathbf{B}\mathbf{R}^{-1}\mathbf{B}^T\mathbf{P}(t)\mathbf{x}_e(t) + \mathbf{E}d + (\mathbf{A}\mathbf{x}_r + \dot{\mathbf{x}}_r), \tag{3-26}$$

where d is the disturbance (for this case $d = mg$). Using Eqs. (3-22), (3-23), and (3-24), the following expression can be obtained

$$\dot{\mathbf{P}}(t)\mathbf{x}_e(t) + \mathbf{P}(t)\dot{\mathbf{x}}_e(t) = -\mathbf{A}^T\mathbf{P}(t)\mathbf{x}_e(t) - 2\mathbf{Q}\mathbf{x}_e(t), \tag{3-27}$$

substituting $\dot{\mathbf{x}}_e(t)$ by the expression given in Eq. (3-26)

$$\dot{\mathbf{P}}\mathbf{x}_e + \mathbf{P}\mathbf{A}\mathbf{x}_e - \frac{1}{2}\mathbf{P}\mathbf{B}\mathbf{R}^{-1}\mathbf{B}^T\mathbf{P}\mathbf{x}_e + \mathbf{P}\mathbf{E}(mg) + \mathbf{P}(\mathbf{A}\mathbf{x}_r + \dot{\mathbf{x}}_r) + \mathbf{A}^T\mathbf{P}\mathbf{x}_e + 2\mathbf{Q}\mathbf{x}_e = 0 \quad (3\text{-}28)$$

which can be reorganized as

$$\left(\dot{\mathbf{P}} + \mathbf{P}\mathbf{A} + \mathbf{A}^T\mathbf{P} - \frac{1}{2}\mathbf{P}\mathbf{B}\mathbf{R}^{-1}\mathbf{B}^T\mathbf{P} + 2\mathbf{Q}\right)\mathbf{x}_e + \mathbf{P}\mathbf{E}(mg) + \mathbf{P}(\mathbf{A}\mathbf{x}_r + \dot{\mathbf{x}}_r) = 0. \quad (3\text{-}29)$$

Because an infinite horizon performance index is selected, $t_f \to \infty$, and $\dot{\mathbf{P}}$ becomes zero. If $\mathbf{P}$ is then selected so that the coefficient of $\mathbf{x}_e$ in Eq. (3-29) is equal to zero, the error $\mathbf{x}_e$ is driven to zero, and the states of the system will follow the desired command. The control law is then given by Eq. (3-25), where $\mathbf{P}$ is the solution of the algebraic Riccati equation [1]

$$\mathbf{P}\mathbf{A} + \mathbf{A}^T\mathbf{P} - \frac{1}{2}\mathbf{P}\mathbf{B}\mathbf{R}^{-1}\mathbf{B}^T\mathbf{P} + 2\mathbf{Q} = 0. \quad (3\text{-}30)$$

In real-world applications there are unknown disturbances to the system that are not included here. Calculations to determine $\mathbf{P}$ were done using the MATLAB (2001) routine *lqry.m* within the control toolbox. Note that the control gains are time-varying and must be determined at each oscillator position.

3.2.4 LQ Tracking Algorithm with State Estimator

Because most of the states of this problem represent generalized coordinates, rather than physical variables, they cannot be measured directly for feedback in a control system. However, to determine the control action, the algorithms used in active and semiactive control require an estimate of the states at any time. To obtain this, an observer that uses measured accelerations from certain points of the beam and the oscillator is used.

Because accelerations are required for feedback, Eq. (2-29) can be reduced so that only the states associated with accelerations become the output of the system.

$$\mathbf{y}_{fb} = \begin{bmatrix}\mathbf{G} & \mathbf{J}\end{bmatrix}\mathbf{x} + \begin{bmatrix}\mathbf{H}_2\end{bmatrix}u(t) + \begin{bmatrix}\mathbf{H}_1\end{bmatrix}(mg). \tag{3-31}$$

Renaming the coefficients of the output equation as

$$\mathbf{C}_{fb} = \begin{bmatrix}\mathbf{G} & \mathbf{J}\end{bmatrix}, \quad \mathbf{D}_{fb} = \begin{bmatrix}\mathbf{H}_2\end{bmatrix}, \text{ and } \quad \mathbf{F}_{fb} = \begin{bmatrix}\mathbf{H}_1\end{bmatrix}. \tag{3-32}$$

so that Eq. (3-31) can be expressed as

$$\mathbf{y}_{fb} = \mathbf{C}_{fb}(t)\mathbf{x} + \mathbf{D}_{fb}(t)u(t) + \mathbf{F}_{fb}(t)(mg) \tag{3-33}$$

For this problem, the observer takes the form

$$\dot{\mathbf{x}}_{es} = \mathbf{A}_o(t)\mathbf{x}_{es} + \mathbf{B}_o(t)u(t) + \mathbf{E}_o(t)(mg) + \mathbf{L}(t)\mathbf{y}'. \tag{3-34}$$

Where $\mathbf{x}_{es}$ is the state vector of the observer. Note the presence of a constant input due to the known mass of the oscillator. Defining

$$\mathbf{y}' = \mathbf{y}_{fb} - \mathbf{D}_{fb}u - \mathbf{F}_{fb}(mg) \tag{3-35}$$

Using Eqs. (3-31) and (3-35) in Eq. (3-34) yields

$$\dot{\mathbf{x}}_{es} = \mathbf{L}\ \mathbf{C}_{fb}\ \mathbf{x} + \mathbf{x}_{es}\mathbf{A}_o + \mathbf{B}_o\ u + \mathbf{E}_o(mg) \tag{3-36}$$

The error between the real and the estimated states is $\mathbf{e} = \mathbf{x} - \mathbf{x}_{es}$. Thus,

$$\dot{\mathbf{e}} = \dot{\mathbf{x}} - \dot{\mathbf{x}}_{es}. \tag{3-37}$$

Substituting the right hand of Eq. (3-37) by the expressions given in Eqs. (2-25) and (3-36) the following error equation is obtained

$$\dot{\mathbf{e}} = (\mathbf{A} - \mathbf{L}\mathbf{C}_{fb} - \mathbf{A}_o)\mathbf{x} + (\mathbf{B} - \mathbf{B}_o)u + (\mathbf{E} - \mathbf{E}_o)(mg) + \mathbf{A}_o\mathbf{e}. \tag{3-38}$$

Defining $\mathbf{A}_o = \mathbf{A} - \mathbf{L}\mathbf{C}_{fb}$, $\mathbf{B}_o = \mathbf{B}$ and $\mathbf{E}_o = \mathbf{E}$, the error becomes

$$\dot{\mathbf{e}} = \mathbf{A}_o\mathbf{e} \tag{3-39}$$

If $\mathbf{L}$ is selected appropriately, the observer will quickly estimate $\mathbf{x}$. In the active control case

$$u(t) = -\frac{1}{2}\mathbf{R}^{-1}\mathbf{B}^T\mathbf{P}(t)(\mathbf{x}_e(t) - \mathbf{x}_{es}(t)), \tag{3-40}$$

and the observer takes the form

$$\dot{\mathbf{x}}_{es} = (\mathbf{A} - \mathbf{L}\mathbf{C}_{fb} - \mathbf{B}\mathbf{K} + \mathbf{L}\mathbf{D}_{fb}\mathbf{K})\mathbf{x}_{es} + (\mathbf{E} - \mathbf{L}\mathbf{F}_{fb})(mg) + \mathbf{L}\mathbf{y}_{fb} \tag{3-41}$$

and the output of the system becomes

$$\mathbf{y} = \mathbf{C}\mathbf{x} + \frac{1}{2}\mathbf{D}\mathbf{R}^{-1}\mathbf{B}^T\mathbf{P}(t)(\mathbf{x}_e(t) - \mathbf{x}_{es}(t)) + \mathbf{F}(mg) \tag{3-42}$$

Calculations to determine $\mathbf{L}$ were done using the MATLAB (2001) routine *lqew.m* within the control toolbox.

3.2.5 Clipped Optimal Control

Using a semiactive device is an attractive alternative to active control for many applications [5, 6, 33, 34]. In this approach for the moving-oscillator problem, the actuator of the semiactive case will replace the regular damper attached to the suspension of the oscillator. The goal of the semiactive control algorithm presented here is to simulate the behavior of an active controller whenever the system and its dynamics allows it. The same linear quadratic tracking algorithm used to calculate the force applied by an active actuator is used herein to provide an optimal response of the semiactive device.

To take full advantage of semiactive devices when applied to civil engineering structures, a clipped optimal control algorithm was developed by Dyke in 1996 [5]. Based on acceleration feedback, this algorithm induces the semiactive device to approximate the behavior of a fully active device whenever the motion of the structure allows it.

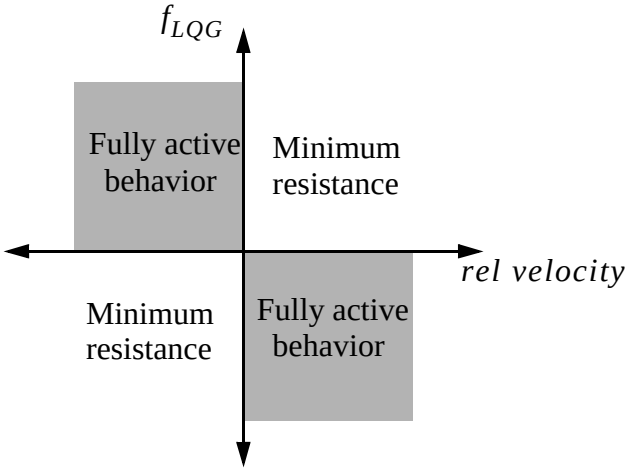

FIGURE 3-3. Graphical representation of force commanded to semiactive devices.

Figure 3-3 shows the desired behavior of the semiactive control device for any values of optimal force calculated by the LQG control algorithm and the relative velocity between the oscillator and the continuum (stroke rate). Thus, the commanded force to the semi-

active device is equal to that of the active case whenever the stroke rate is opposing the required force. For instance, a certain value of optimal tension is commanded only when the damper stroke is increasing, whereas compression is commanded when the stroke is decreasing.

On the other hand, whenever the stroke rate does not oppose the optimal force, the commanded force to the semiactive device is set to zero. As explained in past sections, the damper of variable orifice is set to a minimum value of damping, whereas the voltage of the MR-damper becomes zero. This does not necessarily mean that the actual force applied by the device is zero. In fact, only in rare occasions does this become true.

3.2.5.1 Clipped optimal control algorithm and viscous variable damper

When combined with a viscous variable damper, a clipped optimal control algorithm commands the optimal damping coefficient to the device. At any time, the force applied by the device placed between the oscillator and the continuum is

$$f(t) = c(t)\, v(t), \tag{3-43}$$

where v is the relative velocity between the oscillator and the point of the beam at which the oscillator is placed (stroke rate), and c is the damping coefficient at any time. If f_{COM} is the force commanded by the clipped optimal control algorithm (see section 3.2.4), Eq. (3-43) can be solved for c obtaining the damping coefficient that provides that force

$$c(t) = \frac{f_{COM}}{v(t)} \tag{3-44}$$

It is obviously not possible to provide any value of c required by the control algorithm. For instance, a negative damping coefficient would mean that the damper is introducing external energy to the system, and by definition, a semiactive device is not able to perform this action. On the other hand, these kind of variable dampers have limitations regarding the maximum force they can apply. Thus, an upper limit is also introduced so that the subsystem comprised by the mass of the oscillator, the spring and the damper form a critically damped system.

3.2.5.2 Clipped optimal control algorithm and MR-damper

When a MR-damper is combined with the clipped optimal control algorithm, the commanded signal becomes a voltage rather than a force or a damping coefficient. It is assumed that the force generated by the MR-damper can be measured precisely at any time. Then, the commanded and provided forces are compared.

Several researchers have used bang-bang algorithms to obtain optimal performance from MR-dampers, providing only two possible values of voltage to the semiactive device [11, 34]. By adopting this strategy, a maximum voltage is applied whenever the dissipative force provided by the damper is less than the dissipative force commanded by the LQ algorithm. When this is not the case, the voltage is turned to zero, allowing the damper to flow almost freely. Figure 3-4 provides a schematic representation of this type of algorithm.

Given the rapid dynamics of the MR-damper compared to that of the continuum oscillator system, and after several numerical simulations testing the performance of the bang-bang algorithm, it was found that a great amount of “chattering” may be introduced to the circuit, decreasing dramatically the performance of the control action. This phenomenon occurs when the dissipative force required by the system is greater than the force

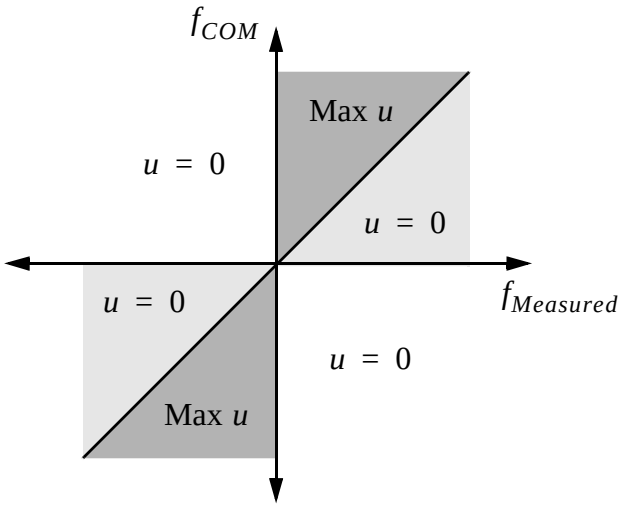

FIGURE 3-4. Bang-bang algorithm for voltage commanded to MR-damper.

provided by the MR-damper, turning the voltage to its maximum value immediately. The force provided then, quickly reaches the desired force, but a great amount of overshoot is provoked. The algorithm then, stops providing the voltage, and therefore, the force quickly drops to a lower value than the required value. This phenomenon takes no longer than tenths or even hundreds of a second and occurs whenever the force required is dissipative and can be provided by a semiactive device.

To minimize this effect in the control algorithm, two different strategies are implemented. First, rather than providing either a maximum voltage or no voltage at all, an increasing or decreasing voltage is commanded to the magnetic field of the device. Therefore, whenever the required force is greater than what is being provided, the voltage will gradually be increased without producing a large amount of overshoot in its response. Obviously a maximum voltage is set before the simulation. Similarly a reduction of the voltage provided is necessary whenever the MR-damper is applying a force of greater value than what it is required. Figure 3-5 schematically displays this proposed solution.

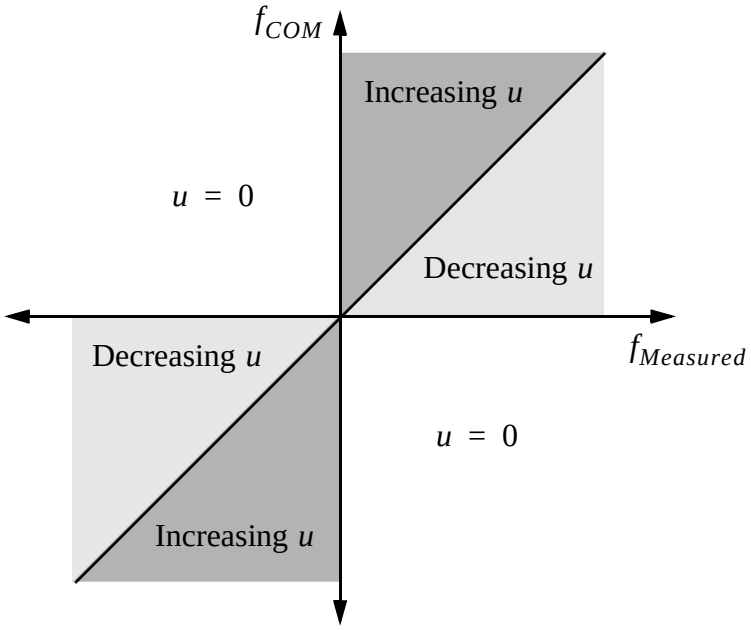

FIGURE 3-5. Graphical representation of voltage commanded to MR-damper.

In addition to the gradual changes in voltage, a low tolerance between the measured and the required forces is introduced to the control algorithm. This means that changes are not introduced to the magnetic field until the required force is significantly different from the one provided. An acceptable value for this tolerance is 5%, which means that the voltage is not increased (or decreased) unless the required force is 1.05 times greater (or smaller) than the force provided at any time. Figure 3-6 displays the difference between the control force provided by algorithms with and without a tolerance value.

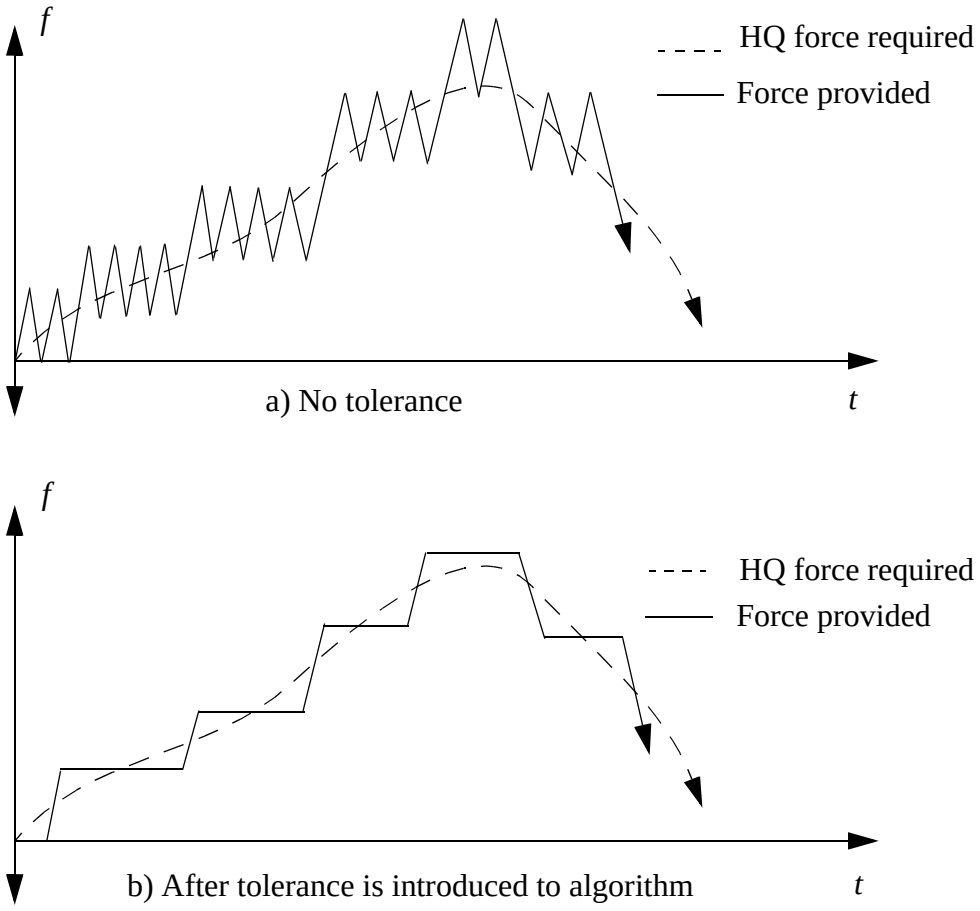

FIGURE 3-6. Schematic difference in algorithms with and without a tolerance value.

3.3 Summary

The mathematical models used to describe the behavior of all devices simulated in this study were defined in this chapter. Advantages, disadvantages and physical limits of those actuators were also discussed here.

The need of a tracking control algorithm that forces the system to have a behavior similar to the quasi-static behavior was explained. Then, based on Green's formula and its derivative, the theoretical quasi-static behavior was found for both the continuum and the oscillator. Finally, all control strategies and algorithms were defined and discussed.

Chapter 4

Control Algorithm Verification

There are several factors that make the problem of controlling the dynamic response of the moving-oscillator model challenging. As mentioned in previous chapters, the variable controllability of the states, and the time dependence of the system are two of the most important difficulties. For this reason, when a control algorithm is numerically evaluated directly on the vehicle-bridge model, the achieved improvements cannot be easily judged. To efficiently test the efficacy of the tracking control algorithm developed in Chapter 3, a simplified model was created. Both the variable controllability of the response, and the time dependency of the system were neglected. An excellent performance of the controlled response was pursued, in order to proceed and apply it to the much more complex moving-oscillator problem.

4.1 The Simplified Model

Figure 4-1 shows the simplified model used for algorithm verification. The lower mass represents the continuum and the upper mass the oscillator. It is obvious that the lower mass cannot represent the full length of the continuum. For instance, if looked at independently, the lower mass has only one natural frequency, whereas the continuum has an unlimited number, each associated with a different mode shape. However, after numerical simulations of the uncontrolled vehicle-bridge model, it was clear that the response

of the continuum was highly dominated by its first mode. For this reason, the lower mass on the simplified model represents only this component of the total response.

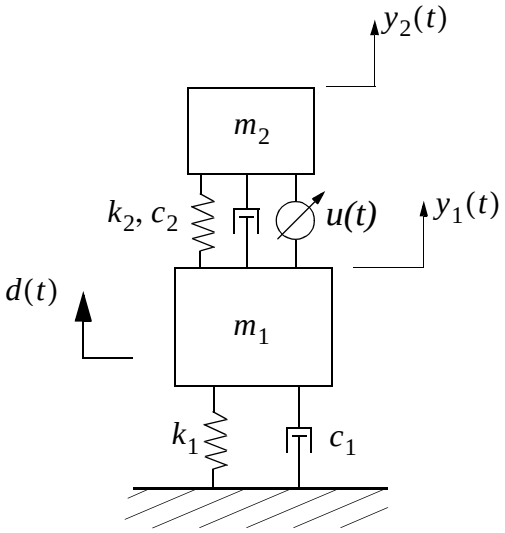

FIGURE 4-1. Simplified model.

The characteristics of this simpler model were then selected to represent the vehicle-bridge problem. Thus, masses, stiffnesses, and damping coefficients were calculated so that the mass ratio and the natural frequencies of the independent subsystems could be compared to those of the system in Chapter 5. $d(t)$, in Fig. 4-1, represents the applied disturbance, $u(t)$ is the control force, and y_1 and y_2 the vertical displacement of the lower and upper mass respectively.

The dynamic equilibrium equations of these two masses are

$$m_1\ddot{y}_1 + (c_1 + c_2)\dot{y}_1 - c_2\dot{y}_2 + (k_1 + k_2)y_1 - k_2y_2 - d + u = 0 \qquad (4\text{-}1)$$

$$m_2\ddot{y}_2 - c_2\dot{y}_1 + c_2\dot{y}_2 - k_2y_1 + k_2y_2 + u = 0 \qquad (4\text{-}2)$$

which, reorganized and expressed in state space form with the state vector $\mathbf{x} = \left[y_1 \; y_2 \; \dot{y}_1 \; \dot{y}_2 \right]^T$, can be expressed as

$$\dot{\mathbf{x}} = \mathbf{A}\mathbf{x} + \mathbf{B}d + \mathbf{E}u, \tag{4-3}$$

where

$$\mathbf{A} = \begin{bmatrix} 0 & 0 & 1 & 0 \\ 0 & 0 & 0 & 1 \\ -\dfrac{(k_1 + k_2)}{m_1} & \dfrac{k_2}{m_1} & -\dfrac{(c_1 + c_2)}{m_1} & \dfrac{c_2}{m_1} \\ \dfrac{k_2}{m_2} & -\dfrac{k_2}{m_2} & \dfrac{c_2}{m_2} & -\dfrac{c_2}{m_2} \end{bmatrix}, \quad \mathbf{B} = \begin{bmatrix} 0 \\ 0 \\ \dfrac{1}{m_1} \\ 0 \end{bmatrix}, \text{ and } \quad \mathbf{E} = \begin{bmatrix} 0 \\ 0 \\ -\dfrac{1}{m_1} \\ \dfrac{1}{m_2} \end{bmatrix}. \tag{4-4}$$

The calculated numerical values are: m_1 = 32000 Kg, m_2 = 4800 Kg, k_1 = 891800 m/N, k_2 = 135000 m/N, c_1 = 3380 $\mathrm{m/(N \cdot sec)}$, and c_2 = 10180 $\mathrm{m/(N \cdot sec)}$.

4.1.1 Tracking Signal

Because the main objective is to control the dynamic response of the continuum (represented by the lower mass in the simplified model), the control algorithm must focus on tracking the states of the pseudo-static response. In addition, because the total response of the continuum is so highly dominated by its first mode, the maximum displacements are present at the midspan. Therefore, the tracking signal contains the displacement and velocity of the continuum's midspan in the pseudo-static case. To calculate this signal, one can substitute $x = \dfrac{L}{2}$ in Eqs. (3-7) and (3-8) obtaining

$$T(t) = -\frac{mgv^2}{3EI}\left(Lt^2 - 2vt^3 + \frac{v^2}{L}t^4\right) \tag{4-5}$$

$$\dot{T}(t) = -\frac{mgv^2}{3EI}\left(2Lt - 6vt^2 + 4\frac{v^2}{L}t^3\right), \tag{4-6}$$

where v is the velocity of the oscillator in the vehicle-bridge system of Chapter 5, L is the length of the continuum, m and EI are the characteristics of the continuum and the oscillator, and g is the gravitational force ($v = 4\ \mathrm{m/s}$, $L = 32\ \mathrm{m}$, $m = 4800\ \mathrm{Kg}$, and $EI = 3\mathrm{e}8\ \mathrm{m}^4/\mathrm{s}^2$).

4.1.2 The Disturbance

The disturbance is applied directly to the lower mass, producing motion in both the upper and the lower mass because of their interaction. This force was chosen to produce a response of the simplified model similar to the response generated by the oscillator as it traverses the continuum. It is composed of two different forces, one a function of the tracking signal, and the second a sinusoidal force.

$$d(t) = d_1(t) + d_2(t) \tag{4-7}$$

The first component applies, at every time, a force of such magnitude that would make the lower mass (m_1) have a static displacement equal to the one being tracked. This does not mean that it will not produce any dynamic response on the system. The expression for this force is

$$d_1(t) = k_1\left(-\frac{mgv^2}{3EI}\left(Lt^2 - 2vt^3 + \frac{v^2}{L}t^4\right)\right). \tag{4-8}$$

For the second disturbance, a sinusoidal force of frequency equal to the natural frequency of the upper mass is applied on the lower one. This force roughly simulates the interacting dynamics present in the moving-oscillator problem. Eq. 4-9 describes this component as

$$d_2(t) = A\sin\left(\sqrt{\frac{k_2}{m_2}}\ t\right), \tag{4-9}$$

where $A = 10000$. Figure 4-2 shows the components and resulting summation of the disturbance.

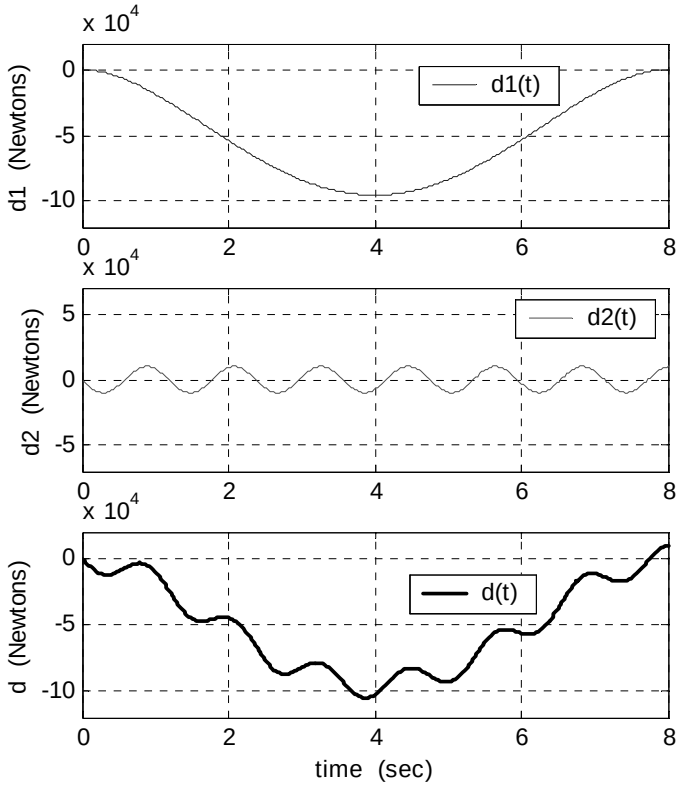

FIGURE 4-2. Disturbance components and total.

4.2 Results

Numerical simulations with an eight second duration are performed to analyze the response of the uncontrolled system and to verify the control algorithms. In the simulations both the upper and the lower mass start at rest (i.e. zero initial conditions).

4.2.1 Uncontrolled Case

Figure 4-3 shows the uncontrolled response of the simplified model. Although the disturbance is applied directly to the lower mass, it produces an amplified response of the upper mass. There are two reasons for this phenomenon. First, the disturbance applied to the system has a sinusoidal component whose frequency is equal to that of the upper subsystem (0.84 Hz, if looked at as an independent subsystem), amplifying its response greatly. However, even more importantly, is the fact that the natural frequencies of the

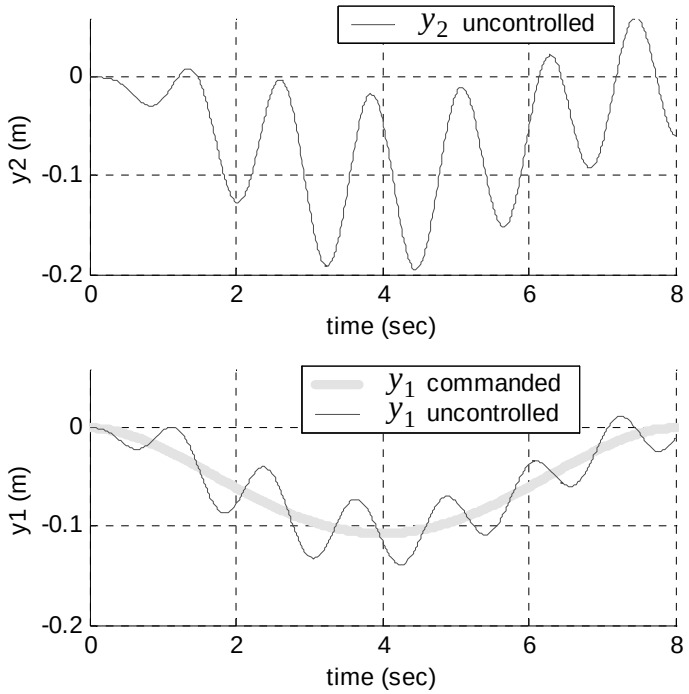

FIGURE 4-3. Uncontrolled behavior.

two masses (as independent subsystems) are very close to each other (approximately 0.84 Hz). Thus, the upper mass reacts to the motion of the lower one in the way a tuned mass damper (TMD) would.

When the upper mass does not have any damping (i.e. $c_2 = 0$) its response is very large, releasing much of the energy that is input by the disturbance, and decreasing the response of the lower mass. For this reason, and unlike the numerical vehicle-bridge model of Chapter 5, an increase on the damping properties of the upper mass (representative of the vehicle) increases the response of the lower mass. Thus c_2 was then selected such that neither mass hit resonance during the simulation (i.e. $\zeta_2 = 20\,\%$).

4.2.2 Active Control Case

For verification purposes, it is assumed that the full state vector can be measured here to obtain the optimal control action. Thus, no estimator is required. The weighting matrix $\mathbf{Q}$ for this simplified model is a square matrix whose size is equal to the number of states (i.e. 4). All but one values are equal to zero. The only numerical value is equal to $1e14$ placed on the first position of its diagonal. This value is associated with the displacement of the lower mass, meaning that only this displacement is weighted, and the force applied controls only this variable. $\mathbf{R}$ is equal to 1.

$$\mathbf{Q} = \begin{bmatrix} 1e14 & 0 & 0 & 0 \\ 0 & 0 & 0 & 0 \\ 0 & 0 & 0 & 0 \\ 0 & 0 & 0 & 0 \end{bmatrix} \tag{4-10}$$

The optimal force is then calculated following the mathematical procedure described in Chapter 3. (section 3.2.3). Figure 4-4 shows the control force applied to the system as a

function of time. Both the controlled and the uncontrolled responses of the lower mass are shown in Fig. 4-5. In addition to those, the commanded displacement (tracking signal) is also shown.

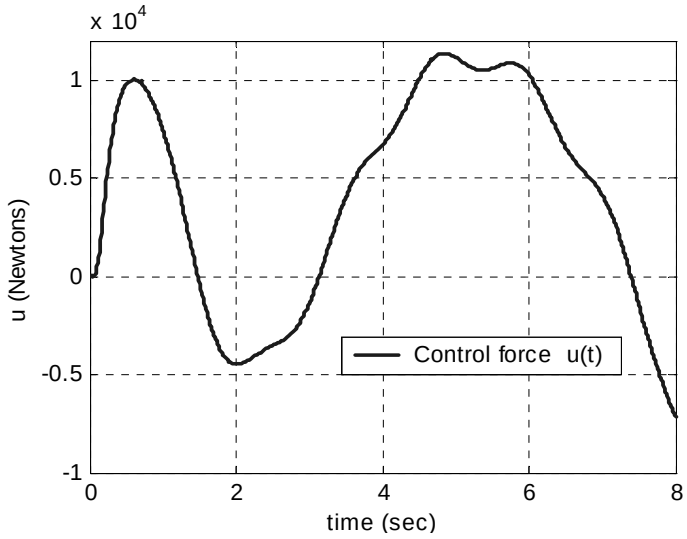

FIGURE 4-4. Active control force.

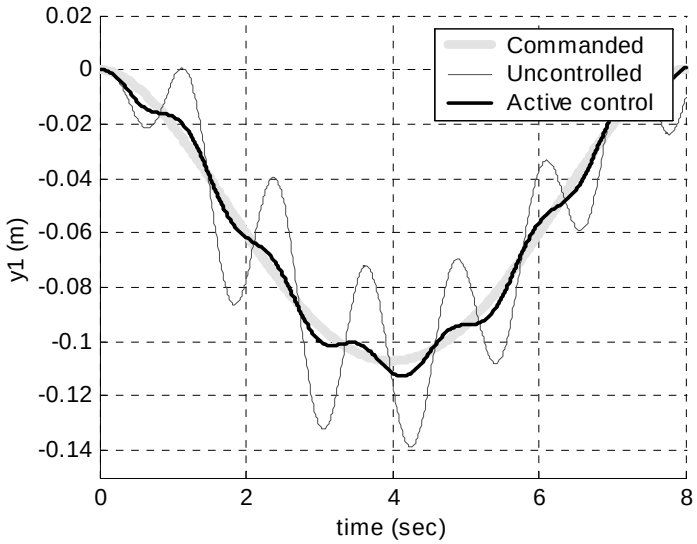

FIGURE 4-5. Response of the lower mass.

An evaluation parameter is defined to compare the behavior of the uncontrolled and the controlled cases with respect to the desired displacement (tracking signal). This evalua-

tion parameter is a measure of the root mean square (RMS) of the difference between the response of the lower mass and the desired displacement over the time frame of interest. This is

$$\sigma_e = \sqrt{\frac{1}{t_f}\int_0^{t_f}(y_1(t) - T(t))^2 dt}, \tag{4-11}$$

where t_f represents the final time of the simulation (8 sec), y_{1i} is the *i*th displacement of the lower mass, and T_i is the *i*th commanded displacement. The result of this evaluation parameter for the uncontrolled case is 0.2829m while the controlled case is 0.0484m. Thus, an improvement of 82.9% is achieved.

The control algorithm, on its current configuration, does not weight the states associated with the upper mass (displacement and velocity), and, on the contrary, uses this mass to generate controlling forces. Therefore, because an aggressive active controller can potentially drive the system unstable, it is important to check the behavior of the upper mass and make sure its response has not been excessively increased. Figure 4-6 shows this response.

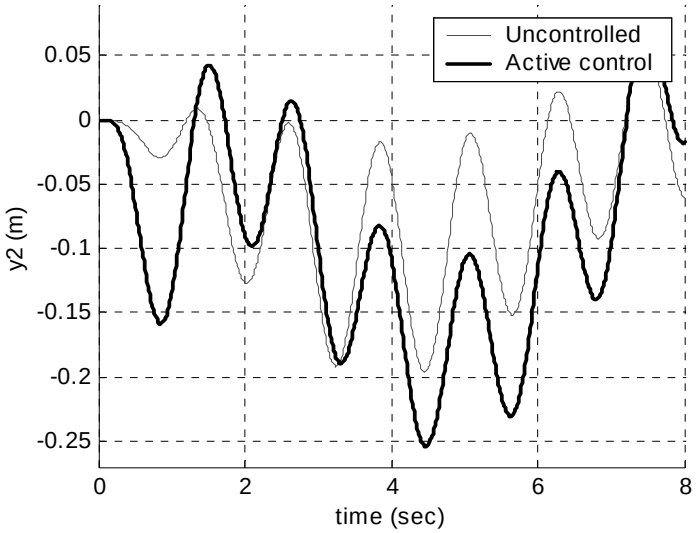

FIGURE 4-6. Response of the upper mass.

Although it is not a goal here, it is preferable to maintain constant the distance between the two subsystems. In the vehicle-bridge model, this would mean that the system does not produce any dynamic response as the oscillator traverses the continuum, having only static displacements at every time. In the simplified model, it would mean that the system is not affected by the second component of the disturbance, and no dynamic response is generated by the first component. For this reason, the evaluation parameter, σ_1, is also useful to quantify the performance of the upper mass with respect to the commanded displacement. After this evaluation, its performance was decreased by only 48%, a trade of somewhat expected after achieving such an excellent performance of the lower mass.

4.2.3 Semiactive Control Case

For the simplified model, only the behavior of the system with a variable orifice damper (described in Chapter 3, section 3.1.2) is analyzed, leaving the MR-damper to be tested with the actual vehicle-bridge model. The optimal control action was determined using the clipped optimal control algorithm described also in Chapter 3 (section 3.2.5). Figure

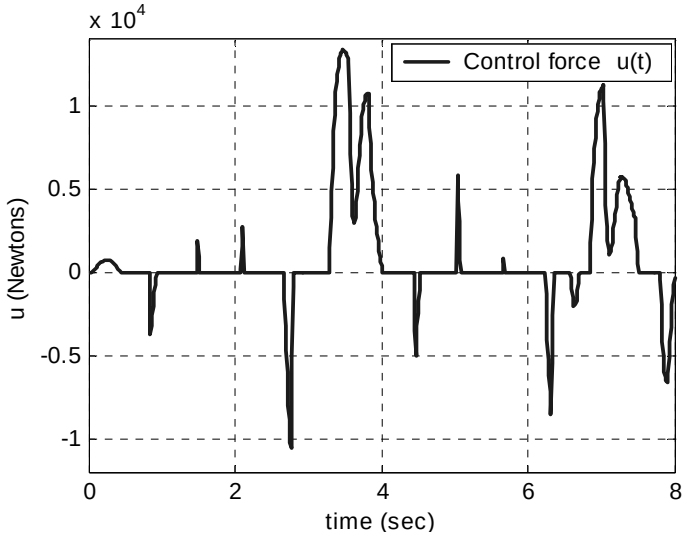

FIGURE 4-7. Semiactive control force.

4-7 shows the forces generated by the device during the simulation, whereas Fig 4-8 shows the response of the lower mass.

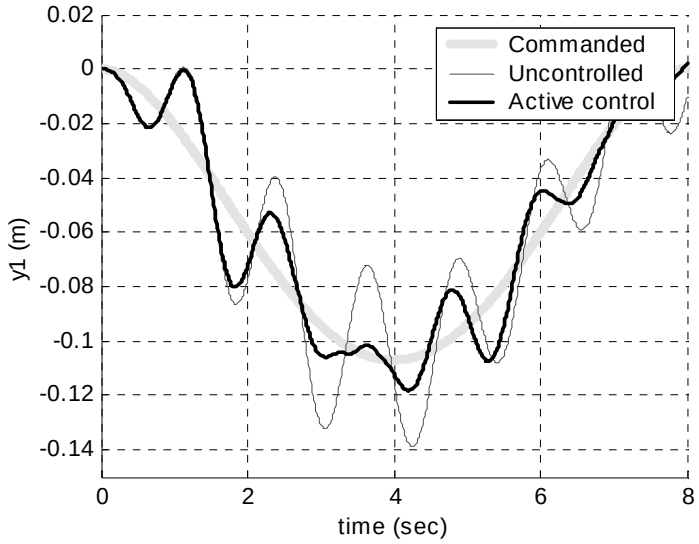

FIGURE 4-8. Lower mass behavior.

The RMS response error of the lower mass with respect to the commanded signal is 0.2829m when no control is applied, whereas a value of 0.1621m is obtained with the semiactive control. Thus, an improvement of 42.7% was achieved. The performance of the upper mass was reduced by 26% only.

4.3 Summary

To verify the tracking control algorithms developed in Chapter 3, a simplified model was considered in this chapter. In this model both the continuum and the oscillator are represented by masses attached to springs, dampers and a single control device. The commanded displacement of the lower mass (representative of the continuum) was obtained from the pseudo-static response of the midspan of the continuum, calculated in Chapter 2.

To better represent the actual vehicle-bridge model, a disturbance was determined and include as an applied force on the lower mass of the model. This force is composed of two components. One of the components is function of the tracking signal, and the other is a sinusoidal force.

Numerical simulations of 8 seconds were performed. Both controlled and uncontrolled responses were found and compare in terms of their RMS values. After evaluating the improvements achieved in the performance of the simplified model, one can conclude that the tracking control algorithm was verified. Both active and semiactive control techniques recorded excellent performances, minimizing the dynamic response of the lower mass without compromising the stability of the system as a whole.

Chapter 5

Numerical Example

To examine the efficacy of the control systems developed in Chapter 3 when applied to the continuum-oscillator problem, a numerical model was created. Numerical simulations with a vehicle-bridge model can confirm that these control techniques are effective regardless of the difficulties brought up by the variable controllability of the states and the variability of the system itself. Several cases were selected to test the robustness of the control systems. The properties of both the continuum and the oscillator were chosen to simulate the interaction between a bridge and a vehicle.

5.1 Properties of the Model

The simply supported Euler-Bernoulli beam model of Chapter 2 is employed in this study. The mass per unit length is defined as ρ and is equal to 1,000 Kg/m. The total length between supports is $L = 32\,\text{m}$, and $EI = 3.0 \times 10^8\,\text{m}^4/\text{sec}^2$. Three modes are used in the eigenfunction expansion that expresses the response of the continuum in terms of its eigenmodes. Damping ratios equal to 2, 4, and 6% are defined for the first, second and third eigenvalues, respectively. The natural frequencies are equal to 0.84, 3.36, and 7.56 Hz.

The oscillator has a mass equivalent to fifteen percent of the total mass of the beam (4800 kg.), a stiffness of $k = 1.35 \times 10^5\,\text{N/m}$, and a constant velocity of $v = 4\,\text{m/sec}$.

Its natural frequency, if considered as an independent subsystem, is equal to 0.84 Hz. The damping coefficient of the oscillator is $c = 509\ \mathrm{N \cdot sec/m}$, which corresponds to a damping ratio of 1% in the uncoupled system.

5.2 Properties and Limitations of the Control Devices

As emphasized in several previous sections of this thesis, the active actuator is assumed to provide instantaneous and precise forces commanded by the LQG control algorithm. Semiactive devices, however, have several limitations inherent to their nature as described in the following sections.

5.2.1 Viscous Damper of Variable Orifice

The force applied by this device is provided by modifying the damping coefficient of the viscous damper placed between the continuum and the oscillator (see Eq. 3-1). For instance, when applied in passive mode, this coefficient is set to a value of $c = 25{,}455\mathrm{N \cdot sec/m}$, that corresponds to a damping ratio of 50% of the oscillator alone. This damping ratio is changed within the range from 1% to 50% based on the force commanded by the clipped optimal control algorithm. Moreover, for all cases, a limit of 3,000N is enforced such that the damping coefficient of the device is changed accordingly if the commanded force surpasses this value.

5.2.2 MR-damper

The parameters of the MR damper were selected so that the device has a capacity of approximately 1,600 N, as follows: α_a = 2.0e5 N/m, α_b = 6.0e4 N/(m·V), c_{0a} = 600 $\mathrm{N \cdot sec/m}$, c_{0b} = 100 $\mathrm{N \cdot sec/m}$, n = 1, A = 12, γ = 3.0e3 $\mathrm{m^{-1}}$, and β = 3.0e3 $\mathrm{m^{-1}}$. These parameters are based on the identified model of a shear-mode prototype MR

damper tested at Washington University [33]. The device was scaled up to reach higher forces required by the vehicle-bridge model.

The voltage commanded to the magnetorheological damper has a range from 0 to 6 volts. Increments (or decrements) of 0.5 volts are applied to the commanded voltage so that the force produced by the device tracks the optimal force calculated by the clipped optimal control algorithm (see Fig. 3-5). However, these changes to the commanded voltage are not applied unless the difference between the required force and the force provided by the device, at any time, is greater than 5% of the latter (see Fig. 3-6).

It is important to note that for those simulations where an MR-damper is tested, no other dissipative device is involved. This means that c becomes zero for those cases, leaving all dissipative forces to be generated by the MR-damper itself.

5.3 Case Studies

To test the efficacy and the robustness of the control techniques, the system is tested under three different conditions of service. In the first set of conditions (denoted Case 1), the beam is in absolute rest at the moment the oscillator enters it, whereas the oscillator moves only horizontally at a constant velocity. Given the high stiffness of the continuum, and the relatively light mass of the oscillator, minimal dynamic interaction could be expected. However, because the natural frequencies of the continuum and the oscillator (if looked at independently) are so close, one can expect increasing interaction when either object is moving.

For the second set of conditions (denoted Case 2), the beam is already excited when the undisturbed oscillator enters it. The initial condition is expressed in terms of the first mode of the beam, and more specifically with the state associated with its displacement (i.e. only q_1 is different than zero). For this case $q_1 = -4$, which means that the dis-

placement at the midspan is equal to 0.14 *m* (downwards), and, at $t = 0$, starts moving upwards to recover its original (rest) position. This initial condition could represent the interaction between the beam and another oscillator right before the oscillator with the control device enters the continuum.

For the third set of conditions a bump is introduced to the problem. A bump may represent an imperfect surface of the continuum, which produces strong disturbance forces into both subsystems. In this particular case, the oscillator hits a sinusoidal bump, as shown in Fig. 5-1. The bump is located at 12.8 meters (40% of the span) from the left support, has a length of 0.64 meters, and reaches 0.5cm from the surface. The location allows the created disturbance to excite all three modes taken into account in the numerical model.

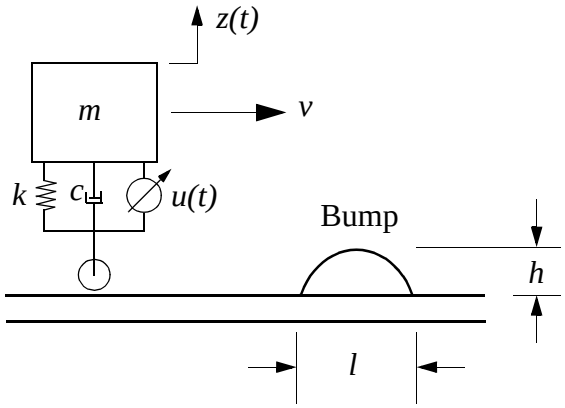

FIGURE 5-1. Sinusoidal bump.

The equation describing the motion of the wheel as it crosses the bump is

$$u_g(t) = h\sin\left(\left(\frac{v}{2l}\right)2\pi\ t\right), \tag{5-1}$$

where l represents the length of the bump, h its height above the surface level, and v the velocity of the oscillator. As the vehicle crosses the bump the disturbance force applied to both subsystems is

$$f_{dist}(t) = m\,\ddot{u}_g(t), \tag{5-2}$$

where m represents the mass of the oscillator. Under the third set of conditions, and similarly to the second set, some initial conditions are imposed to the system, while combining the disturbance generated by the bump. Table 5-1 summarizes all three cases.

TABLE 5-1. Summary of cases studied.

Case	Initial conditions	Bump
Case 1	Zero	No
Case 2	Non-zero	No
Case 3	Non-zero	Yes

5.4 Evaluation Criteria

To compare the performance achieved with all control techniques, five evaluation criteria were chosen. Both displacements and accelerations of the two subsystems are then quantified and numerically compared.

As emphasized in Chapter 1, the main goal of this study is to minimize the dynamic response of the continuum. Therefore, to properly compare the effectiveness of the different control techniques to reduce displacements of the continuum, the pseudostatic response is calculated and removed from the actual response of the system. The pseudostatic response is calculated using Green's formula, discussed in Chapter 3 (Eq. 3-7).

Although none of the control algorithms are set to apply any control action to reduce accelerations, it is important to evaluate their behavior and ensure no large impulses are

generated by the control force. Moreover, because most of the control techniques applied in this study use semiactive dampers that dissipate energy in a controlled way, accelerations are expected to be reduced. Accelerations are analyzed at two different points of the beam, ensuring all three modes are considered.

Similarly, the response of the vehicle is also quantified to guarantee its displacements are not largely increased by the control force. Given the fact that the vehicle is the only body that the control devices can "hold on to" in order to apply a control force to the continuum, its displacements are not expected to be reduced by the control action. Because of the external energy that the active control can input to the system, the displacements of the oscillator may become a critical factor for this technique. Pseudostatic displacements are also subtracted from the oscillator's response.

To examine numerically the behavior of accelerations and displacements, a measure of the root mean square (RMS) responses over the time frame of interest is computed. This is defined as

$$\sigma_i = \sqrt{\frac{1}{t_f}\int_0^{t_f} (r(t))^2 dt} \tag{5-3}$$

where σ_1 is the ith evaluation parameter, t_f represents the final time of the simulation (8 sec), and r is the parameter to be evaluated. For instance, when accelerations are to be evaluated $r(t) = a_i(t)$, where a is the acceleration at any time and the subindex i represents the number of the accelerometer. If displacements are to be evaluated then $r(t) = w(L/2, t) - T(L/2, t)$, where $w(L/2, t)$ is the displacement at the midspan as a function of time, and $T(L/2, t)$ is the tracking signal (pseudostatic displacement) of the midspan.

TABLE 5-2. Summary of evaluation criteria.

Parameter	Evaluation Criteria	Position
σ_1	RMS of accelerations	25 %
σ_2	RMS of accelerations	50 %
σ_3	RMS of relative displacements	50 %
σ_4	Peak of absolute displacements	50 %
σ_5	RMS of relative displacement	Oscillator

Finally, the maximum absolute displacement of the continuum is evaluated for each of the control techniques. Table 5-2 summarizes all evaluation criteria considered.

5.5 Uncontrolled Behavior

Before performing the controlled simulations, it is important to understand the dynamics and behavior of the coupled system as the oscillator traverses the continuum. Because the system is time-varying, the natural frequencies of the system change as the oscillator changes its position and the distribution of the mass is different. Figure 5-2 shows the variation of these frequencies. Note that at $x = 0$ and $x = L$ the system is decoupled, and, when the oscillator is at these points, the frequencies are those of each independent system. Also, notice that, for the parameters selected, the natural frequency of the oscillator is very close to the first mode of the continuum.

While higher frequencies of the continuum vary only slightly with the position of the oscillator, the first mode varies significantly. Its frequency changes 31.3% from the decoupled value. The natural frequency corresponding to the oscillator varies 23.6% as compared to the frequency of the oscillator alone. These important changes constitute the reason to calculate different control gains at every time step. Most civil engineering structures with an active or semiactive control system are considered to be time invariant, and therefore, only one calculation of gains is required. However, because the vehi-

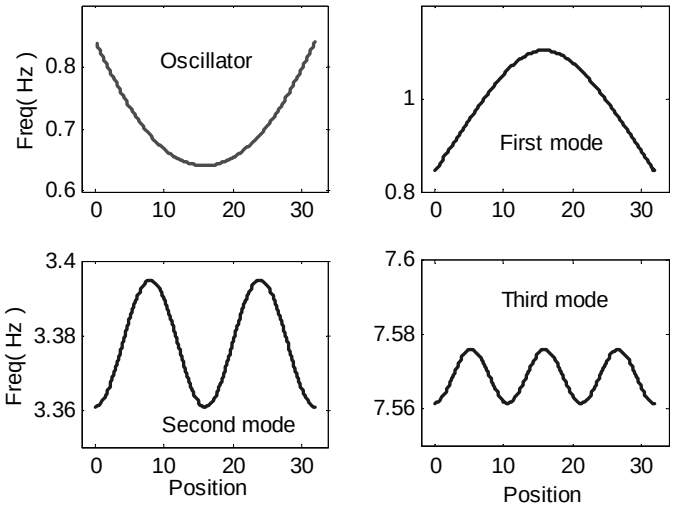

FIGURE 5-2. Variation of the system frequencies as oscillator traverses continuum.

cle-bridge model have changes as high as 31% (depending on the continuum/oscillator mass ratio), time-varying gains become a necessity to apply an accurate control action and make sure the system is not driven unstable.

After evaluating numerical simulations of the uncontrolled system using the mathematical model described in Chapter 2, it became clear that the response of the beam is strongly dominated by its first mode. In fact, there is a ratio of approximately 17 to 1 of the response of the first mode with respect to the second one. The ratio with respect to the third mode is approximately 86 to 1. Based on this knowledge, the control algorithms were designed by weighting only the generalized coordinate associated with the first mode of the continuum, q_1.

Figure 5-2 provides the response of the uncontrolled system (in terms of its states). Here, the states z_1 and $\dot{z_1}$ represent the displacement and velocity of the oscillator and are given in m and m/sec respectively, whereas the states q_{ith} and $\dot{q}_{ith}$ are associated with the i^{th} mode of the continuum and, because they do not represent any physical response, are dimensionless.

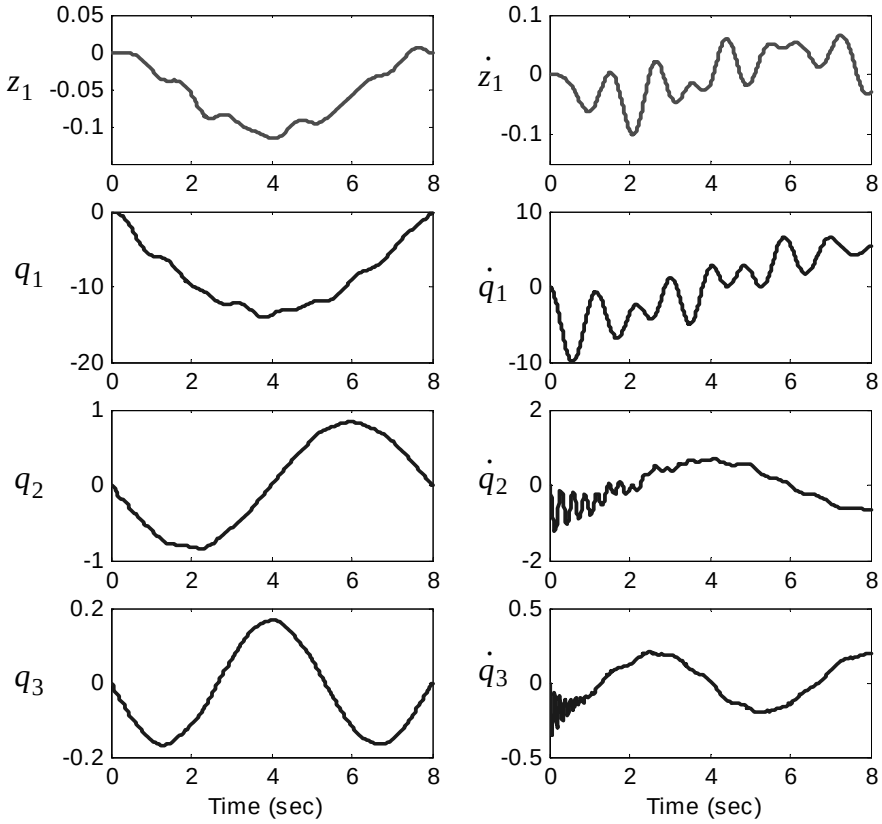

FIGURE 5-3. Uncontrolled behavior with no initial conditions.

5.6 Controlled Results

A total of five controlled simulations were performed for each case considered. The response of the system with both of the semiactive devices was analyzed under two conditions: i) commanded by their optimal algorithm, and ii) set to their passive mode (i.e., $c = 25455\ \mathrm{N \cdot sec/m}$ for the damper of variable orifice, and $V = 6$ Volts for the case of the MR- damper). Table 5-3 shows a summary of all simulations performed, the technique used, the control device and algorithm, and the information used for feedback.

TABLE 5-3. Summary of simulations performed

Technique	Actuator	Control Algorithm	Feedback
Uncontrolled	None	None	None
Active control	Active	LQG	Acceleration
Semiactive control	Variable damper	Clipped optimal	Acceleration
Passive control	Variable damper	None	None
Semiactive control	MR-damper	Clipped optimal	Acceleration
Passive control	MR-damper	None	None

The performance of each system is compared to the behavior of the uncontrolled system in terms of the evaluation criteria described, stating the improvement with respect to this case in percentage values. The reduction of each parameter is defined as

$$\text{Reduction (\%)} = \frac{\sigma_{i(\text{uncontrolled})} - \sigma_{i(\text{controlled})}}{\sigma_{i(\text{uncontrolled})}} \times 100 . \qquad (5\text{-}4)$$

For all control algorithms, a diagonal weighting matrix, $\mathbf{Q}$, was used with a value 1×10^6 associated with the first mode of the continuum. As mentioned before, this controller considers time-varying control gains. Thus, it is assumed that the controller knows the location of the oscillator at each time.

5.6.1 Case 1: Results

Accelerations at two different points of the beam are provided in Fig. 5-4. Notice that peak accelerations are reached during the first second, when the control device has little influence over the system. This is especially true in both of the semiactive cases (variable damper and MR-damper), which do not make any changes to the suspension of the oscillator until the first second has passed. It is clear that the accelerations of the active and semiactive controlled cases are damped out much faster than in the uncontrolled case. However, the difference between the semiactive cases and their respective passive modes (variable damper set at its maximum damping coefficient, and maximum voltage

of the MR-damper) cannot be easily visualized. For instance, when comparing the RMS values (provided in Table 5-4), the performance of both of the semiactive cases outperformed the passive cases by only 8% at the midspan of the beam (σ_2).

As emphasized before, no controllers are designed specifically to reduce accelerations. Thus, the improvements achieved are due to the reduction of the overall dynamic response of the system.

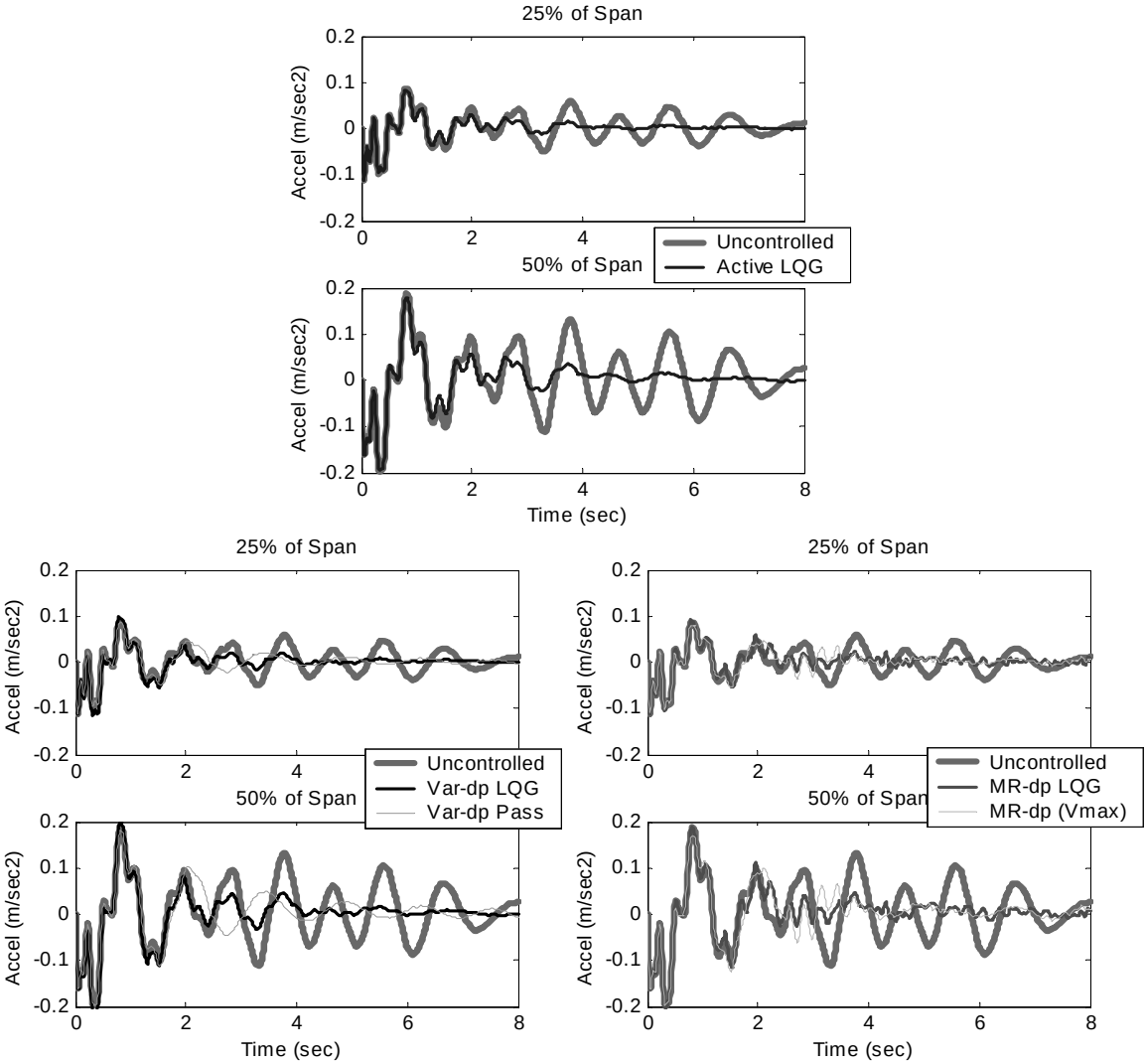

FIGURE 5-4. Accelerations of the continuum. (Case 1)

When the two subsystems are undisturbed at the moment the oscillator enters the beam, the dynamic interaction between these two makes the beam reach a maximum displacement at the midspan 5.5% greater than that calculated with a pseudostatic analysis. Figure 5-5 provides the time history of the deflections of the continuum at this point, once the pseudostatic deflections were removed (referred to as the relative displacements). The reduction of the RMS values of this evaluation parameter is 29.8% with the active actuator commanded by the LQG control algorithm, and 24.6% and 22.5% with the variable damper and the MR-damper respectively (when commanded by the clipped optimal control algorithm). These improvements are much higher than those achieved with the

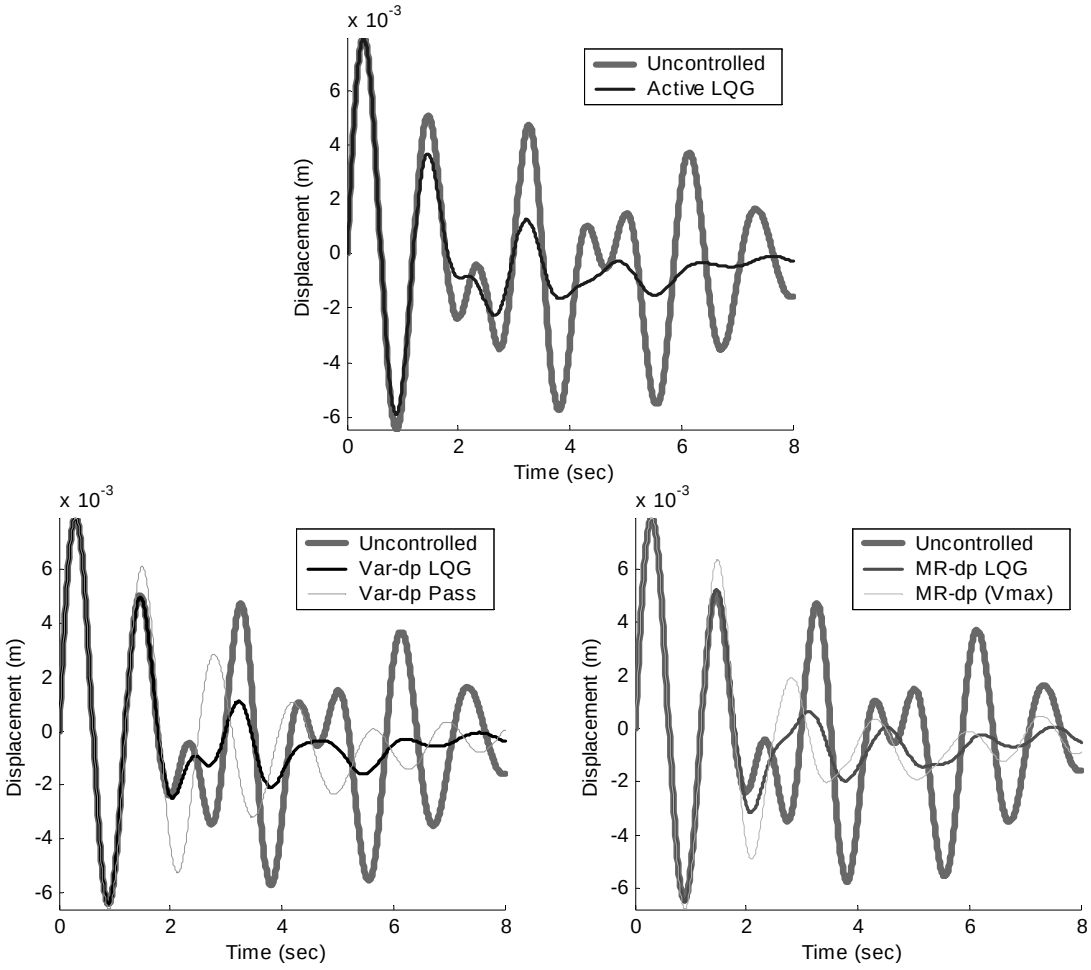

FIGURE 5-5. Mid-span relative displacement vs. time. (Case 1)

semiactive devices in their passive mode: 10.1% and 13.4% with variable damper and MR-damper, respectively (see σ_3, provided in Table 5-4).

Figure 5-6 shows the relative displacement of the oscillator (with respect to the pseudo-static reponse) for the uncontrolled and the actively controlled cases. As experienced with the simplified problem discussed in Chapter 4, the displacement of the oscillator was not expected to be reduced by the action of an active actuator. However, as seen in Fig. 5-6, the response of the vehicle is increased only during the first two seconds of the simulation. The reason for this phenomenon is the low controllability of the first mode of the continuum when the oscillator is near any of the supports, which increases the required control forces to minimize the continuum's displacements. As a result, the much lighter mass of the oscillator is negatively affected. Once those two critical seconds have passed, the overall dynamic response of the system has already been reduced greatly, and even the oscillator's displacements are significantly decreased.

Because no external energy can be input by the semiactive devices, the performance of the oscillator was expected to surpass the performance achieved with the active controller. The highest reduction of the vehicle's displacement is achieved by the MR-damper

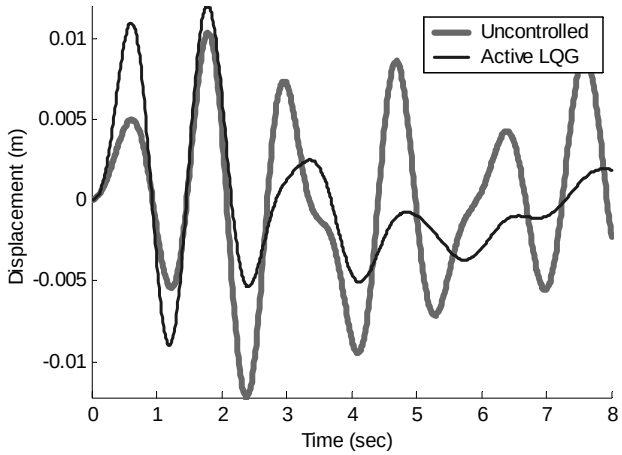

FIGURE 5-6. Oscillator relative displacement vs. time. (Case 1)

commanded by the clipped optimal control algorithm, which, in terms of its RMS value, is reduced by 38.8% (see σ_5, provided in Table 5-4).

Very similar reductions of the peak absolute displacement are achieved by all control techniques. Table 5-4 provides the summary of all evaluation parameters and the improvements achieved with respect to the uncontrolled case.

TABLE 5-4. Evaluation criteria for Case 1.

Actuator	**Uncont.**	**Acitve**	**Variable damper**		**MR-damper**	
Algorithm	**None**	**LQG**	**CO***	**None**	**CO***	**None**
σ_1	0.0701	0.0475	0.0546	0.0552	0.0521	0.0552
Reduction (%)		32.3	22.1	21.2	25.7	21.3
σ_2	0.0909	0.0589	0.0644	0.0698	0.0642	0.0697
Reduction (%)		35.2	29.2	23.2	29.4	23.3
σ_3	0.0031	0.0022	0.0024	0.0028	0.0024	0.0027
Reduction (%)		29.8	24.6	10.1	22.5	13.4
σ_4	0.1125	0.1086	0.1089	0.1085	0.1087	0.1080
Reduction (%)		3.5	3.2	3.5	3.3	3.9
σ_5	0.0053	0.0043	0.0034	0.0037	0.0032	0.0045
Reduction (%)		18.6	35.2	29.9	38.8	15.0
* CO = Clipped Optimal						

5.6.2 Case 2: Results

Case 2 considers a bridge that is already excited when the vehicle traveling at a constant velocity approaches. The most important reason to analyze the performance of the control techniques with this set of conditions is to test their efficacy under normal working conditions that a vehicle-bridge system may be exposed to. As expected, a much larger dynamic interaction between the two subsystems occurs when the beam is initially excited by previous traffic (as implied in this case).

Unlike active actuators, the capacity of semiactive devices is limited by the interaction of the two subsystems. Thus, the larger the interaction between the continuum and the oscillator, the larger the effect of the device can be. For this reason, the action of both of the semiactive devices was expected to greatly minimize the overall dynamic response of the system under the set of conditions imposed in Case 2. As seen in Fig. 5-7, and similar to the first case (where no initial conditions were imposed), similar accelerations are obtained with all control techniques during the first two seconds of the simulations.

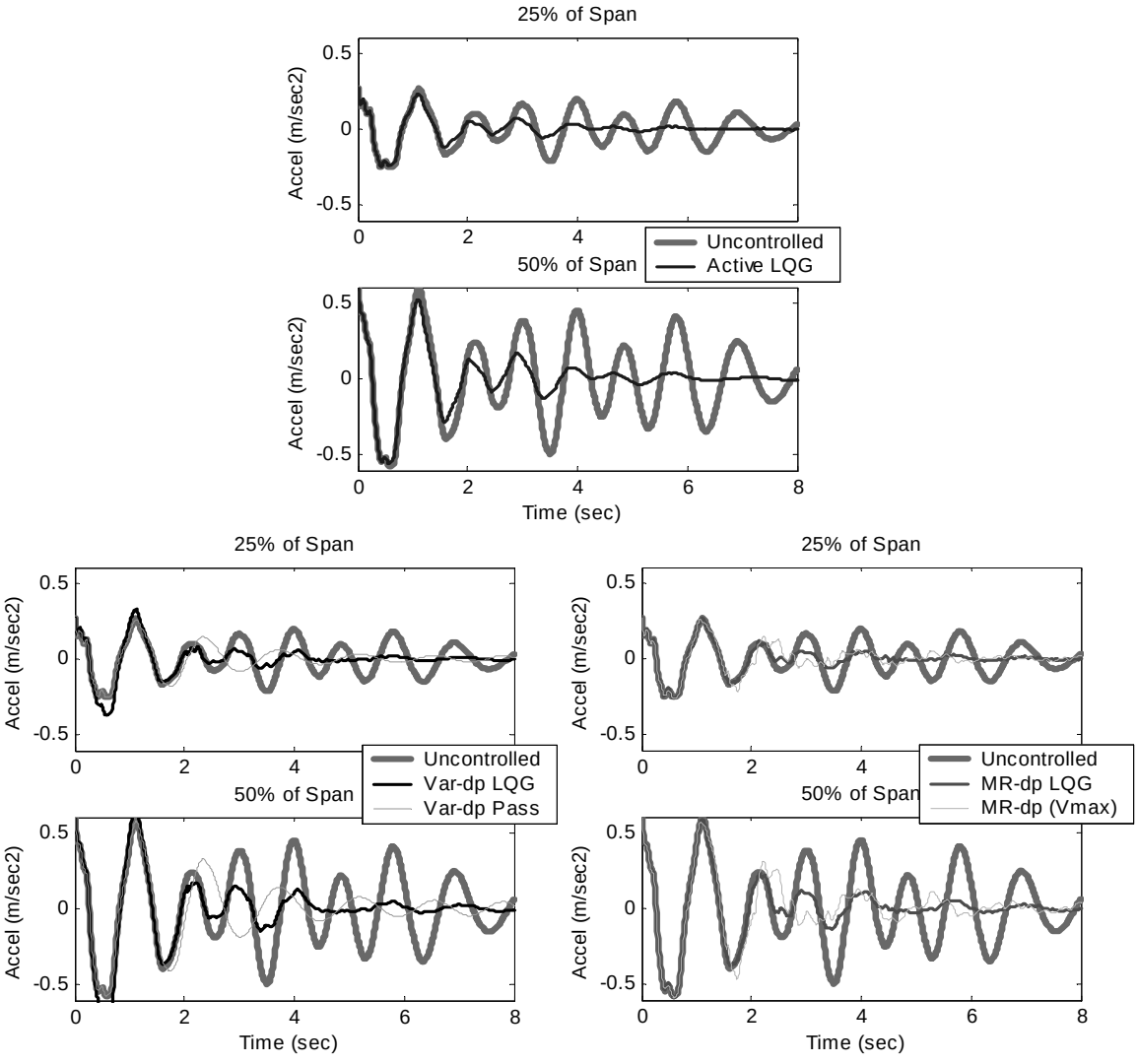

FIGURE 5-7. Accelerations of the continuum. (Case 2)

Clearly, both active and semiactive systems are very effective in reducing accelerations of the model after this short period of time. However only marginal improvements with respect to the passive modes are achieved. In fact, when comparing the RMS value of accelerations, similar results are obtained for both semiactive and passive modes.

As seen in Fig. 5-8 large reductions of the midspan displacement are achieved by both active and semiactive devices, outperforming the uncontrolled and the passive cases. Surprisingly however, a large reduction was achieved by the MR-damper when set to its

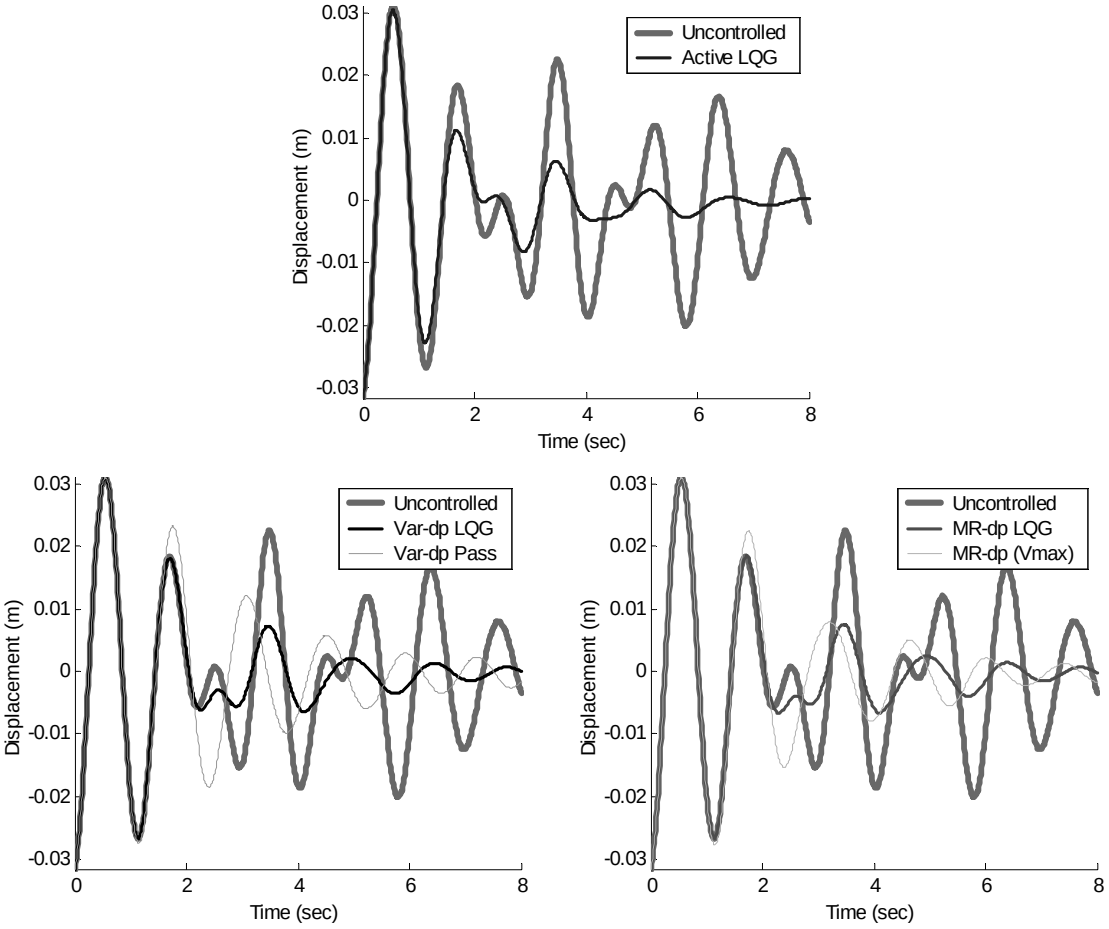

FIGURE 5-8. Mid-span relative displacement vs. time. (Case 2)

maximum voltage, being outperformed by its semiactive mode by only 11% (see σ_3, provided in Table 5-5).

Figure 5-9 shows the displacements of the oscillator (after pseudostatic displacements are subtracted) for the uncontrolled and actively controlled cases. Similar to the behavior of this evaluation criteria in Case 1, its amplitude was increased only during the first two seconds of the controlled simulation, after which it was greatly reduced. The maximum reductions of the RMS values of this displacements were achieved by the semiactive devices when set to their passive modes. For instance, the improvement achieved by the variable damper was 55.7%, with respect to the uncontrolled case, outperforming the reduction of the semiactive mode, 39.4%. A similar situation occurred with the MR-damper.

A remarkable reduction of the maximum absolute displacement of the continuum was achieved by most control techniques. The highest reduction was the result of the active control action, which decreased it by 12.5%, whereas both of the semiactive systems achieved a reduction of about 10%. Table 5-5 provides a summary of all evaluation criteria and their improvements with respect to the uncontrolled case.

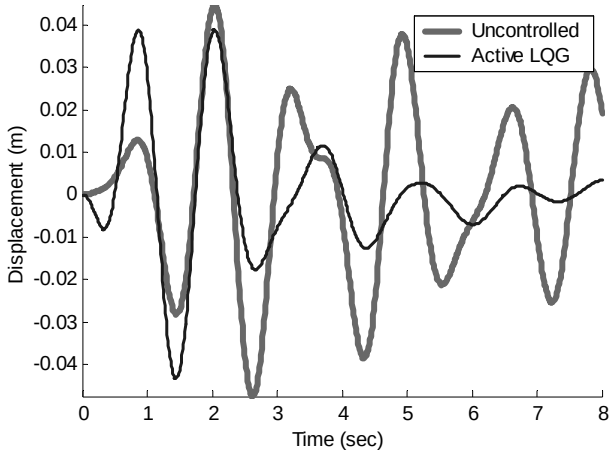

FIGURE 5-9. Oscillator relative displacement vs. time. (Case 2)

TABLE 5-5. Evaluation criteria for Case 2.

Actuator	Uncont.	Acitve	Variable damper		MR-damper	
Algorithm	**None**	**LQG**	**CO***	**None**	**CO***	**None**
σ_1	0.2735	0.1728	0.2147	0.2078	0.1907	0.2018
Reduction (%)		36.8	21.5	24.0	30.3	26.2
σ_2	0.3708	0.2384	0.2652	0.2803	0.2598	0.2711
Reduction (%)		35.7	28.5	24.4	29.9	26.9
σ_3	0.0130	0.0088	0.0098	0.0114	0.0099	0.0109
Reduction (%)		31.9	24.2	11.8	23.6	15.7
σ_4	0.1258	0.1101	0.1134	0.1165	0.1136	0.1150
Reduction (%)		12.5	9.8	7.3	9.7	8.6
σ_5	0.0208	0.0148	0.0126	0.0092	0.0127	0.0107
Reduction (%)		28.9	39.4	55.7	39.3	48.5
* CO = Clipped Optimal						

5.6.3 Case 3: Results

Case 3 considers the introduction of a bump that represents an uneven surface of the continuum, as well as an initially excited system. It is important to emphasize that in this case, the state estimator ignores the characteristics of the bump, making the problem a challenge in this sense. Figure 5-10 shows both the real and the estimated first four states as the oscillator traverses the continuum. Note that after the oscillator hits the bump (at $t = 3.2$ sec), the estimator requires approximately a second to reach, again, a good estimation of the states. An inaccurate estimation of the states can, potentially, lead to apply an inadequate control force increasing the dynamic response of the system.

Usually, a control system is designed to perform best for a certain estimated level of disturbance. For instance, to select the best possible design, a wide range of matrices $\mathbf{Q}$ was used for the first two sets of conditions (modifying its aggressiveness), knowing that no external disturbance was being applied to the system other than the weight of the

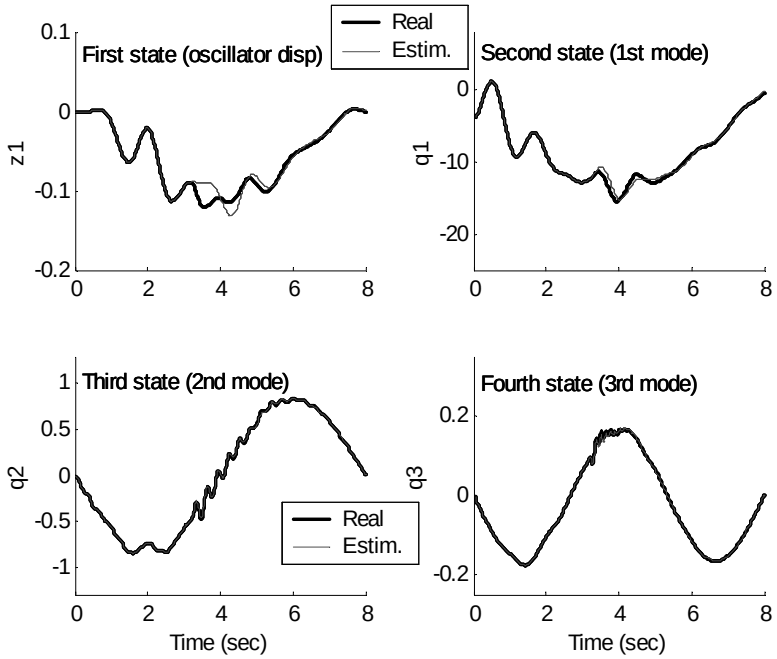

FIGURE 5-10. Comparison of real vs. estimated states (Case 3)

oscillator itself. However, what makes this third case more challenging is the fact that the level of disturbance changes dramatically for a short period of time (0.16 sec), during which the oscillator is in contact with the bump.

One way to overcome this problem is to increase the aggressiveness of the control system during the time the disturbance is introduced by the uneven road. After all, the assumption of knowing the exact position of the oscillator was already made, and assuming a known position of a bump is not out of reach. However, the lack of an accurate estimation of the states shortly after the bump makes this solution unrealizable. In fact, this would mean that an even larger and miscalculated control force could be introduced to the system, most likely, increasing its dynamic response.

Using state feedback simulations (no estimator) combined with high authority controllers during a short period of time after the disturbance of the bump is introduced, showed that the optimal response of the controller (to a bump of the characteristics used

here) is always a large dissipative force that opposes the disturbance. This, in the active control case, means that a much larger force is required for this period of time. In both of the semiactive cases their maximum capacity was reached ($c = 25455\ \mathrm{N \cdot sec/m}$ for the variable damper, and $V = 6$ Volts for the MR-damper). For this reason the original clipped optimal algorithm was modified to produce these values for a short period of time (three times the time required for the oscillator to cross the bump). By modifying the control algorithm, inappropriate control forces, resulting form the poor estimation of the states, are not allowed to be introduced to the system, giving the estimator some time to "recover" from the bump.

Figure 5-11 shows the forces applied by the control devices commanded by their optimal algorithms with the modification explained before. Notice how the variable damper reaches its maximum capacity (3000 N) shortly after the bump has been hit by the oscillator. Because no changes were made to the algorithm that commands the active actuator, the difference on the forces applied by this actuator and the semiactive devices can easily be noticed at the time the oscillator hits the bump ($t = 3.2$ sec).

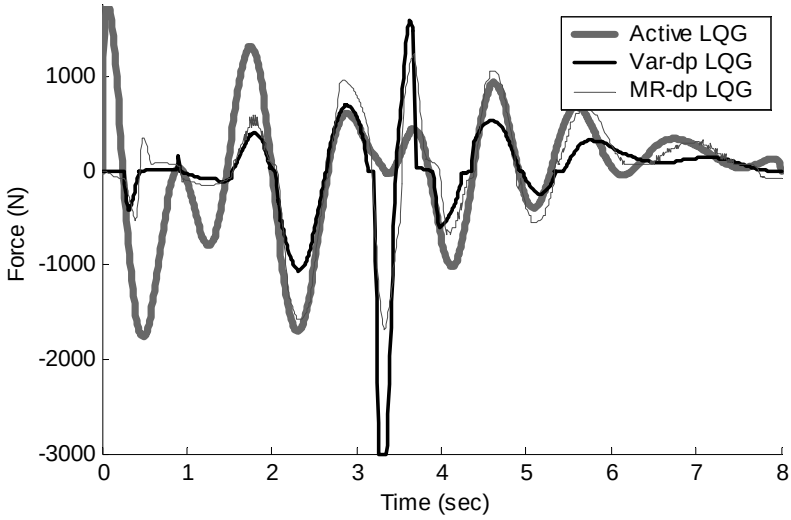

FIGURE 5-11. Control forces applied. (Case 3)

Figures 5-12 and 5-13 give us an idea of the magnitude of the disturbance produced by the bump. For the uncontrolled cases, the existence of the bump increases the displacement of the midspan by 29%. Both velocities and accelerations are also increased dramatically when this disturbance is introduced. As seen in Fig. 5-12, no major reductions of accelerations were achieved by any of the semiactive devices commanded by their modified clipped optimal algorithms, with respect to their passive modes.

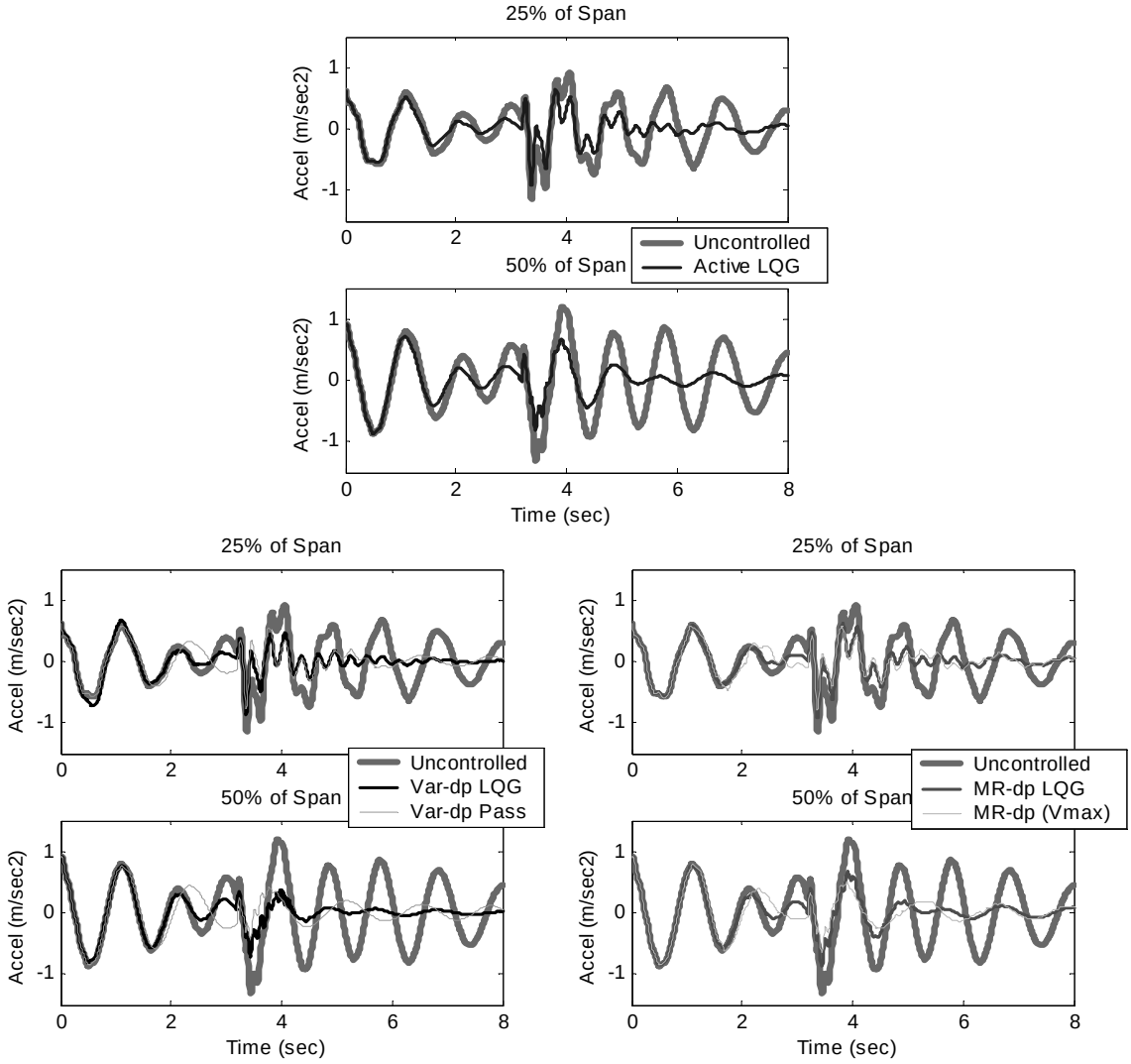

FIGURE 5-12. Acceleration of the continuum. (Case 3)

If only the responses of the system after the bump were analyzed and compared, both of the semiactive devices, commanded by their modified clipped optimal control algorithms, would outperform the active controller. This can be easily seen in Fig. 5-13 (for $t > 3.2$ sec). However, because the action of the active controller minimizes the response of the system in the "pre-bump" period so much quicker than the semiactive devices, the overall performance is similar (see σ_3 for the active and semiactive cases provided in Table 5-6).

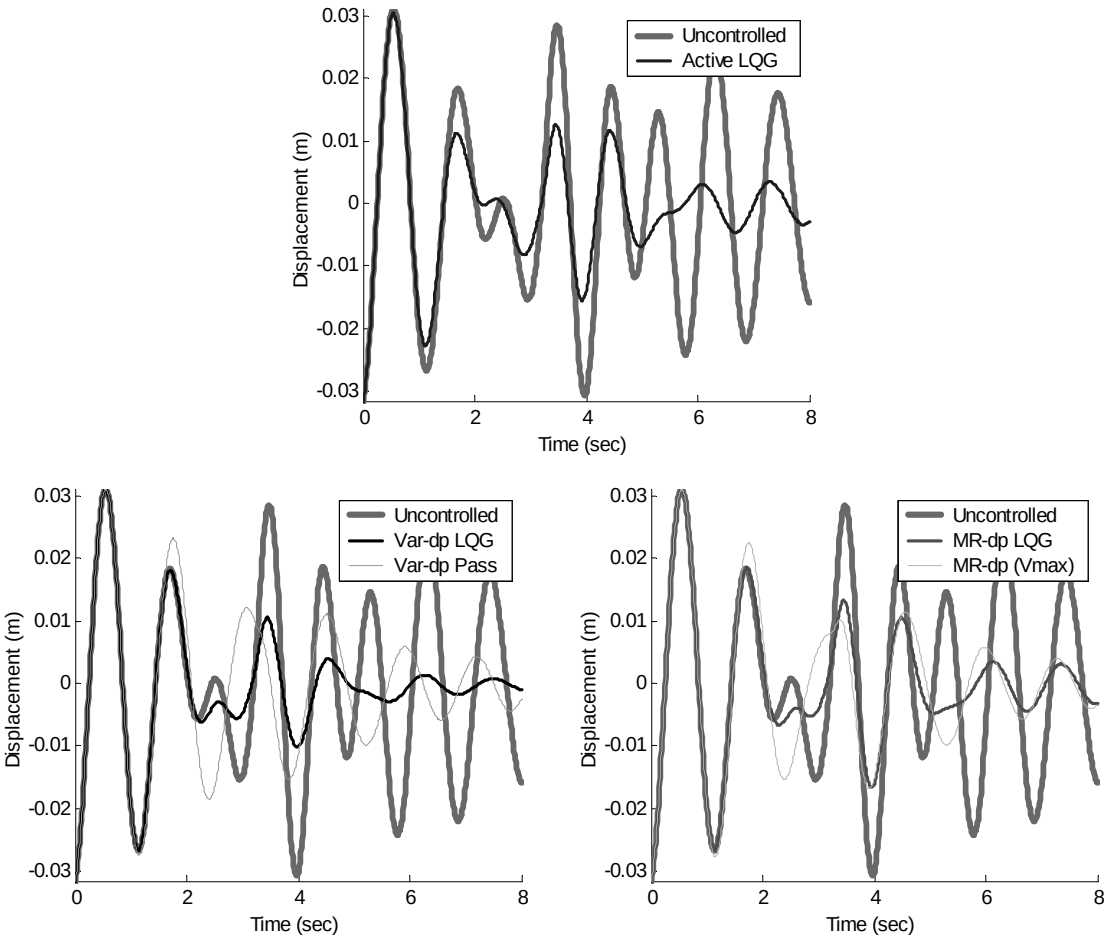

FIGURE 5-13. Mid-span relative displacement vs. time. (Case 3)

Figure 5-14 shows the relative displacement of the oscillator for the uncontrolled and actively controlled cases. Similar to Cases 1 and 2, this displacement was increased dramatically during the initial 25% percent of the span, Table 5-6 provides all evaluation parameters for this set of conditions.

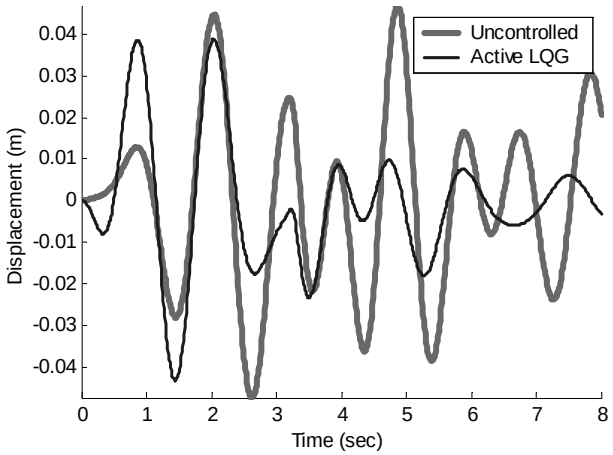

FIGURE 5-14. Oscillator relative displacement vs. time. (Case 3)

TABLE 5-6. Evaluation criteria for Case 3.

Actuator	**Uncont.**	**Acitve**	**Variable damper**		**MR-damper**	
Algorithm	**None**	**LQG**	**CO***	**None**	**CO***	**None**
σ_1	0.4090	0.2409	0.2461	0.2407	0.2476	0.2406
Reduction (%)		41.1	39.8	41.2	39.5	41.2
σ_2	0.5527	0.3092	0.2866	0.3115	0.3232	0.3134
Reduction (%)		44.1	48.1	43.6	41.5	43.3
σ_3	0.0157	0.0098	0.0100	0.0121	0.0107	0.0118
Reduction (%)		37.6	36.2	22.8	31.6	24.4
σ_4	0.1377	0.1225	0.1172	0.1222	0.1237	0.1238
Reduction (%)		11.0	14.9	11.3	10.2	10.1
σ_5	0.0216	0.0156	0.0123	0.0109	0.0129	0.0123
Reduction (%)		27.6	43.0	49.3	40.0	42.7
* CO = Clipped Optimal						

5.7 Summary

To verify the efficacy and robustness of the control algorithms developed in Chapter 3, several control scenarios were examined. The properties of both the continuum and the oscillator were chosen to simulate the interaction between a full scale bridge and vehicle. All properties and limitations of the devices used to apply controlling forces were also modeled and discussed herein.

Three different cases were defined. For the first case, an initially undisturbed system was selected. In Case 2, nonzero initial conditions were imposed on the system. For the final case, the already initially disturbed system was increased in complexity by adding a bump, that represents an uneven surface. A small variation of the clipped optimal control algorithm was created to accommodate the problem of the partially unknown disturbance created by the bump.

The uncontrolled response of the system and the variability of its natural frequencies as the oscillator traverses the continuum were analyzed. Based on this analysis, it was decided to design the control algorithms to focus on minimizing the first mode of the beam. The importance of having a variable controller was demonstrated.

Five evaluation criteria were defined to properly compare the performance of all control techniques. Root mean square (RMS) values of accelerations at two points of the continuum, the midspan displacement, and the oscillator's displacement were among those parameters. The displacement values, however, were calculated after the pseudostatic response of the system was calculated and subtracted from the actual response.

Similar reductions in displacements of the continuum were achieved by both active and semiactive techniques, outperforming uncontrolled and passively controlled systems. Only marginal reductions of accelerations were obtained with semiactive control tech-

niques as compared to those achieved with passive techniques. Both variable damper and MR-damper were very effective in reducing the displacements of the oscillator.

Chapter 6

Conclusions and Future Work

Active and semiactive control techniques were proposed in this thesis to minimize the dynamic response of an elastic continuum when traversed by a moving oscillator. The first step was to derive the mathematical model that describes the time varying dynamics of the system. Then, a tracking control algorithm that uses a quadratic performance index and acceleration feedback was developed. This algorithm was appropriately modified to take full advantage of each of the three control devices chosen to perform the control action. A simplified model was used to successfully verify the efficacy of the tracking algorithm developed. Then, a full scale vehicle bridge model was created and used to perform both controlled and uncontrolled simulations. Comparisons of the performance of the different control techniques to reduce the dynamic response of the system were based on a set of evaluation criteria. Performances achieved with semiactive techniques were similar to those achieved with active control, while requiring only a fraction of the power used by an active actuator. Both active and semiactive systems outperformed passive techniques.

As discussed in Chapter 5, all control strategies focused on reducing the response of the first mode of the continuum, and more specifically, the state associated with its displacement. As a result, important reductions of the RMS values of the continuum's midspan relative displacements were achieved by both active and semiactive control systems. Poor performance of passive techniques was observed.

Although not specifically pursued by any of the control systems, important reductions in the oscillator's relative displacement were achieved by all control techniques. Experience gained with the simplified model of chapter 4, in which the displacements of the upper mass (representative of the vehicle) increased, indicated we should not expect good results regarding this response. However, when applied to the vehicle-bridge model, the overall response of the system was reduced in such a way that even the oscillator's response was decreased. Moreover, because of their inability to introduce external energy to the system, both semiactive and passive systems (which performed similarly) highly outperformed the active control regarding this evaluation criterion.

Similar to the case of the oscillator's displacement, accelerations of the continuum were greatly reduced with respect to the uncontrolled case, even though the control algorithms were not focused on reducing this aspect of the response. Again semiactive and passive techniques performed similarly, but were both outperformed by the active control in most cases.

As expected, the performance achieved with the MR-damper and with the variable orifice damper, when commanded by their optimal algorithms, were very similar, the latter being slightly more efficient in all cases. This result is due to the ideal model assumed to simulate the variable damper, which gives the device the capacity to precisely track the optimal force commanded by the control algorithm (whenever this force is dissipative). However, when set to their passive modes, the MR-damper performed consistently better than the variable damper.

As demonstrated through the results herein, the performance of the passive systems is always better than the uncontrolled case. Thus, if any control action is to be taken without a good estimation of the states, it is preferable to apply passive control rather than applying an inaccurate control force or no control force at all. For this reason, the modification made to the control algorithms for Case 3 (bump present) improved the results

obtained with the semiactive techniques compared to those obtained with active control. However, an external disturbance of different characteristics than a bump (whose location and properties can be easily determined) is possible in a vehicle-bridge system. Other alternatives must be then considered.

Remarkable tracking capabilities of the commanded force of the MR-damper were achieved by introducing the changes to the algorithm that control the voltage provided. A great amount of “chattering” inherently produced by a bang-bang algorithm was avoided by introducing the small increments (or decrements) on the voltage, and setting minimum tolerance between the commanded and provided forces.

Some restrictions apply to the control algorithms developed in this thesis. For instance, one assumption was the fact that only vehicles traveling at a moderate velocity were considered, allowing the continuum to deflect statically and producing an overall dynamic response that oscillates about the pseudostatic response. Under this condition, the tracking algorithm performs properly as demonstrated with the numerical example created in Chapter 5. However, for vehicles traveling at a high velocity, the overall dynamic response of the continuum does not approach the pseudostatic response, and further study is needed for these situations. In addition, for fast-moving oscillators, minimal interaction between the two subsystems occurs, limiting the control action of semiactive devices.

Future Work

One further direction in this research could be to consider several oscillators with different properties, including velocities, masses, suspension characteristics, entering times and even control capabilities. Even though previous traffic was considered in Cases 2 and 3, no interaction with other oscillators was considered. Simulations of this nature

require much more computing effort and small variations on the mathematical model to include the states associated with the new subsystems.

Analyzing the behavior of the stresses of the continuum is an important factor to take into account in future research. Pesterev and Bergman proposed a method that overcomes the difficulty of expressing the non-continuous shear-force functions in terms of the continuous shape functions used to describe the behavior of the beam [25]. Including the force generated by the control device into this method could be a possibility to achieve this objective.

Several issues regarding the capabilities of the data acquisition system shall be addressed in future research. For instance it was assumed in this study that accelerations were perfectly measured using sensors along the continuum and the oscillator. However, in real applications, noise in sensors is a factor that control systems should account for. Moreover, the event of missing one or more signals from the sensors should also be considered.

References

[1] Brogan, W.L. 1991. *Modern Control Theory,* Prentice Hall. Upper Saddle River, New Jersey. pp. 501–521.

[2] Bureau of Transportation Statistics (1997). *Truck Movements in America: Shipments from, to, within and through States*. Technical Report BTS/97-TS/11, Washington D.C., U.S. Govt. Printing Office.

[3] Chen, C.H. and Wang, K.W., 1994. "An Integrated Approach Toward the Modeling and Dynamic Analysis of High-Speed Spindles, Part II: Dynamics Under Moving End Load" *J. Vibr. and Acoustics*, ASME, V 116, pp. 514–22.

[4] Chopra, A.K. 1995. *Dynamics of Structures*, Prentice Hall. Upper Saddle River, New Jersey. pp. 586–593.

[5] Dyke, S.J. (1996), "Acceleration Feedback control Strategies for active and Semi-active Control Systems: Modeling, Algorythm Development, and Experimental Verification," *Ph.D. Dissertation*, Department of Civil Engineering and Geological Sciences, University of Notre Dame, Indiana.

[6] Dyke, S.J., B.F. Spencer, Jr., M.K. Sain and J.D. Carlson (1996). "Modeling and Control of Magnetorheological Dampers for Seismic Response Reduction," *Smart Materials and Struc.,* Vol. 5, pp. 565–575.

[7] Dyke, S.J., Johnson, S.M. 2001. "Active Control of a Moving Oscillator on an Elastic Continuum." *Proc. of the Structural Safety and Reliability Conf.* (in press).

[8] Dyke, S.J., B.F. Spencer, Jr., Sain, M.K., and Carlson, J.D. 1996a. "Modeling and Control of Magnetorheological Dampers for Seismic Response Reduction," *Smart Materials and Struc.,* Vol. 5, pp. 565–575.

[9] Dyke, S.J., Spencer Jr., B.F., Quast, P., Sain, M.K., Kaspari Jr., D.C. and Soong, T.T., 1996b. "Acceleration Feedback Control of MDOF Structures," *Journal of Engineering Mechanics,* ASCE, Vol. 122, No. 9, pp. 907–918.

[10] Dyke, S.J., Spencer Jr., B.F., Quast, P., Kaspari Jr., D.C., and Sain, M.K., 1996c. "Implementation of an AMD Using Acceleration Feedback Control," *Microcomputers in Civil Engrg.*, Vol. 11, pp. 305–323.

[11] Dyke, S.J., Spencer Jr., B.F., Sain, M.K. and Carlson, J.D. (1998). “An Experimental Study of MR Dampers for Seismic Protection,” *Smart Materials and Struc.: Special Issue on Large Civil Structures*. Vol. 7, pp. 693–703.

[12] Giraldo, D., and Dyke, S.J. 2002. “Control of a Moving Oscillator on an Elastic Continuum Using Smart Dampers.” *Proc. of the American Control Conference*, Anchorage, Alaska.

[13] Guo, W.H. and Xu, Y.L. 2000. “Direct Assembling Matrix Method for Dynamic Analysis of Coupled Vehicle-Bridge System.” *Proc. of the Adv. in Struc. Dyn. Conf.*, Elsevier Science, Ltd., Vol. I, pp. 513–520.

[14] Iwan, W.D. and Moeller, T.L., 1976. “The Stability of Spinning Elastic Disk With a Transverse Load System” *J. of Applied Mech., ASME,* Vol 43, pp. 485–90.

[15] Iwan, W.D. and Stahl, K.J., 1973. “The Response of an Elastic Disk with a Moving Mass System.” *J. of Applied Mech., ASME,* Vol 40, pp. 445–51.

[16] Karnopp, D. 1990. “Design Principles for Vibration Control Systems Using Semi-Active Dampers,” *J. of Dynamic Systems, Measurement, and control*, ASME, Vol 112, September 1990, pp. 448–455.

[17] Katz, R., Lee, C.W., Ulsoy, A.G., and Scott, R.A., 1987. “Dynamic Stability and Response of a Beam Subject to a Deflection Dependant Moving Load.” *ASME J. of Vibr., Acoustics, Stress, and Rel. in Design*. Vol. 109, pp. 361-65.

[18] Katz, R., Lee, C.W., Ulsoy, A.G., and Scott, R.A. 1987. “The Dynamic Response of a Rotating Shaft Subject to a Moving Load,” *J. Sound and Vibr.*, V. 122, No. 1, pp. 131–48.

[19] Kim, C.W. and Kawatani, M. 2000. “Analytical Investigation for Vehicle-Bridge Interaction Between Dynamic Wheel Loads and Bridge Response.” *Proc. of the Adv. in Struc. Dyn. Conf.*, Elsevier Science, Ltd., Vol. I, pp. 391–398.

[20] Lynch, J.P., Law, K. H., Kiremidjian, A.S., Kenny, T., and Carrier, E. 2002. “A Wireless Modular Monitoring System for Civil Structures,” *Proc. of the Int. Modal Analysis Conf.*, Los Angeles, CA., Feb. 2002.

[21] Nassif, H. Liu, M., and Ertekin, O. 2002. "Development of a Bridge Dynamic Load Model Using Computer Simulation," *Proc. of the Structural Safety and Reliability Conf*, New Port Beach, CA., Feb. 2002.

[22] Omenzetter, P. and Fujino, Y. 2000. “Modeling of Vehicle-Bridge Interaction as MDOF Oscillator Moving over 1D Continuum.” *Proc. of the Adv. in Struc. Dyn. Conf.*, Elsevier Science, Ltd., Vol. I, pp. 415–422.

[23] Pesterev, A.V. and Bergman, L.A. 1997a. “Response of an Elastic Continuum Carrying Moving Linear Oscillator.” *J. of Engrg. Mech.*, ASCE, August 1997, pp. 878–84.

[24] Pesterev, A.V. and Bergman, L.A. 1997b. “Vibration of Elastic Continuum Carrying Accelerating Oscillator.” *J. of Engrg. Mech.*, ASCE, August 1997, pp. 886 – 889.

[25] Pesterev, A.V., Bergman, L.A., and Tan, C.A. 2000. “Response and Stress Calculations of an Elastic Continuum Carrying Multiple Moving Oscillators.” *Proc. of the Adv. in Struc. Dyn. Conf.*, Elsevier Sci., Ltd., Vol. I, pp. 545–552.

[26] Sadek, F. and Mohraz B. 1998. “Semiactive Control Algorythms for Structures With Variable Dampers,” *J. of Engrg. Mech.*, ASCE, Vol 124, No 9, pp. 981–989.

[27] Shen, I.Y., 1993. “Response of a Stationary, Damped, Circular Plate Under a rotating Sliding Bearing System,” *J. Vibr. and Acoustics*, ASME, Vol. 115, pp. 65–69.

[28] Spencer Jr., B.F. and Sain, M.K. 1997. “Controlling Buildings: A New Frontier in Feedback,” *IEEE Control Syst. Mag.* (Tariq Samad G. Ed.), Vol. 17, No. 6, pp. 19–35.

[29] Soong, T.T. 1990. “Active Structural Control: Theory and Practice,” Longman Scientific and Technical, Essex, England.

[30] Soong, T.T. and Skinner, G.K. 1981. “Experimental Study of Active Structural Control,” *J. of Engrg. Mech.*, ASCE, Vol 113, No 6, pp. 1057–1067.

[31] Yang, B., Tan., C.A., and Bergman, L.A. 1998. “On the Problem of a Distributed Parameter System Carrying a Moving Ocsillator,” *Dyn. and Control of Dist. Systems* (H. Tzou and L.A. Bergman eds.). Cambridge University Press, Cambridge, United Kingdom, Vol. I, pp. 69–94.

[32] Yang, B., Tan, C.A., and Bergman, L.A. 2000. “Direct Numerical Procedure for Solution of Moving Oscillator Problems.” *J. of Engrg. Mech.*, ASCE, Vol. I, pp. 462–469.

[33] Yi, F., Dyke, S.J., Caicedo, J.M., and Carlson, J.D. 2001. “Experimental Verification of Multi-Input Seismic Control Strategies for Smart Dampers,” *J. of Engrg. Mech.*, ASCE, Vol 127, No 11, pp. 1152–1164.

[34] Yoshida, O., Dyke, S.J., Giacosa, L.M. and Truman, K.Z. "Torsional Response Control of Asymmetric Buildings Using Smart Dampers," *Proc. of the 15th ASCE Engrg. Mech. Conf.,* New York, NY, June 2-5, 2002.

[35] Zhu, W.D. and Mote, C. D., Jr. 1987. “Free And Forced Response of an Axially Moving String Transporting a Damped Linear Oscillator,” *J. Sound and Vibr.*, Vol. 177, No. 5, pp. 591–610.

Vita

Diego Giraldo

EDUCATION

- Washington University, St. Louis, MO, M.S: Civil Engineering, 2002
- Universidad del Valle, Colombia, South America: B.S. Civil Engineering, 1998

PROFESSIONAL HISTORY

- *Research Assistant* – Washington University Structural Control & Earthquake Engineering Laboratory, St. Louis, Missouri (January 2001–present)
- *Construction Inspector* – Bimbo de Colombia, Cali, Colombia, South America (April 1999 – June 1999).
- *Construction Instructor* – Servicio Nacional de Aprendizaje SENA, Cali, Colombia, South America (May 1998 – February 1999).

AFFILIATIONS

- Earthquake Engineering Research Institute
- Mid America Earthquake Center

December 2002

Short Title: Control of the Moving-Oscillator Problem, Giraldo, M.S., 2002